AEDC-TR-67-131

THE SPECTRAL REFLECTANCE OF WATER AND CARBON DIOXIDE CRYODEPOSITS FROM 0.36 TO 1.15 MICRONS

B. E. Wood, A. M. Smith, and B. A. McCullough

ARO, Inc.

August 1967

AEROSPACE ENVIRONMENTAL FACILITY
ARNOLD ENGINEERING DEVELOPMENT CENTER
AIR FORCE SYSTEMS COMMAND
ARNOLD AIR FORCE STATION, TENNESSEE

NOTICES

When U. S. Government drawings specifications, or other data are used for any purpose other than a definitely related Government procurement operation, the Government thereby incurs no responsibility nor any obligation whatsoever, and the fact that the Government may have formulated, furnished, or in any way supplied the said drawings, specifications, or other data, is not to be regarded by implication or otherwise, or in any manner licensing the holder or any other person or corporation, or conveying any rights or permission to manufacture, use, or sell any patented invention that may in any way be related thereto.

Qualified users may obtain copies of this report from the Defense Documentation Center.

References to named commercial products in this report are not to be considered in any sense as an endorsement of the product by the United States Air Force or the Government.

THE SPECTRAL REFLECTANCE OF WATER AND CARBON DIOXIDE CRYODEPOSITS FROM 0.36 TO 1.15 MICRONS

B. E. Wood, A. M. Smith and B. A. McCullough
ARO, Inc.

AF - AEDC
Arnold AFS Tenn

FOREWORD

The research reported herein was sponsored by Arnold Engineering Development Center (AEDC), Air Force Systems Command (AFSC), under Program Element 6144501F, Project 8951, Task 895104.

The results of the research were obtained by ARO, Inc. (a subsidiary of Sverdrup & Parcel and Associates, Inc.), contract operator of AEDC, AFSC, Arnold Air Force Station, Tennessee, under Contract AF 40(600)-1200. The work was performed during the period from 1 May 1965 through 1 May 1967 under ARO Project No. SW5703, and the manuscript was submitted for publication on June 2, 1967.

The authors would like to acknowledge R. C. Birkebak of the University of Kentucky and J. D. Haygood of ARO, Inc. for their helpful suggestions concerning this work.

This technical report has been reviewed and is approved.

Terry L. Hershey
Captain, USAF
Research Division
Directorate of Plans
and Technology

Edward R. Feicht
Colonel, USAF
Director of Plans
and Technology

ABSTRACT

The spectral reflectances of water and carbon dioxide cryodeposits were measured in a vacuum integrating sphere as a function of angle of incidence, substrate material, and cryodeposit thickness. Both Cat-a-lac® black paint and a polished copper surface were used as substrates. Measurements were made for wavelengths between 0.36 and 1.15 μ. Cryodeposit thicknesses ranging from 0 to 2.5 mm were investigated. For large cryodeposit thickness, the reflectance was, in general, increased considerably, especially for a Cat-a-lac black substrate. For thin cryodeposit thicknesses of less than 10 μ, interference patterns were observed. A computer program was written to calculate the energy reflected from cryodeposits for 6000°K blackbody irradiation. The reflectance data obtained in the present experiments may be useful for application to thermal models of planetary surfaces such as those of Mars and Venus.

CONTENTS

APPENDIXES

I. ILLUSTRATIONS

Figure

NOMENCLATURE

A_c	Area of the cryosurface, cm^2
B_{MgO}	Detector output from light being first incident on the MgO, mv
B_S	Detector output from light being first incident on the sample, mv
C_1	Constant = 3.7413×10^{-12} w-cm^2
C_2	Constant = 14,388 μ-°K
c	Velocity of light, cm/sec
D	Density of cryodeposit, gm/cc

d	Thin film thickness, μ
$E(\lambda, T)$	Spectral emittance
$F(x_i)$	Fraction of total energy between $x = \infty$ and $x = x_i$
$f(x_i)$	Fraction of total energy between $x = 0$ and $x = x_i$
$f(\lambda_{12})$	Fraction of total energy between wavelengths λ_1 and λ_2
h	Planck's constant
$J(\lambda_1, \lambda_2, T)$	Emissive power
k	Boltzmann constant
ℓ_{av}	Calculated average thickness of the cryodeposit, mm
m	Order of interference
$\dot{m}$	Mass flow rate of test gas, gm/sec
N	Normal to the surface
n	Index of refraction
T	Temperature, °K
t	Time
x	Variable equal to $\frac{C_2}{\lambda T}$
$\Delta\omega_i$	Solid angle containing incident radiation
θ'	Angle of refraction in refracting media, deg
λ	Wavelength, μ
ρ_{MgO}	Reflectance of magnesium oxide
ρ_s	Sample reflectance
ψ	Angle of incidence (measured from the normal), deg

SECTION I
INTRODUCTION

In recent years the field of aerospace simulation has increased steadily in degree of complexity. Attempts are being made to simulate nearly every known aspect of the space environment. Some of the factors being considered are the vacuum environment, solar and particulate radiation, micrometeoroids, and the radiative heat sink of the star background. This latter factor is approximately equivalent to a 4°K blackbody. At present, thermal radiation and vacuum are the environments most often simulated in space chambers. It may be readily shown that chamber walls maintained at liquid-nitrogen (LN_2) temperature (77°K) closely approximate the 4°K radiative temperature of space for most thermal balance test purposes. These walls are coated with black paint to maximize the absorption of radiation incident on them, since in space any radiation leaving the vehicle never returns. However, the 77°K walls will cryopump condensable gases present in the chamber, thereby forming frosts on the black surfaces. These frosts will alter the wall reflectance. For accurate heat balance measurements, this change in wall reflectance must be considered. Since water (H_2O) and carbon dioxide (CO_2) will be the most abundant condensable gases, the reflectances of these frosts are of most importance.

In addition to space simulation considerations, the visible and near-infrared spectral reflectances of H_2O and CO_2 frosts are also of interest in determining planetary environments. In particular, the optical characteristics of these frosts are useful in analyses of the polar caps of Mars and the clouds of Venus (Refs. 1, 2, and 3). Since the frosts considered in this investigation were formed under conditions comparable to these planetary environments, the results presented here may be helpful in planetary studies.

This report presents the reflectances of H_2O and CO_2 cryodeposits as a function of wavelength, angle of incidence, substrate material, and cryodeposit thickness. The wavelength range considered was from 0.36 to 1.15 μ. Approximately 71 percent of the total energy from a 6000°K blackbody lies in this wavelength region. The H_2O and CO_2 deposits were formed on a surface coated with Cat-a-lac® black paint and on a polished copper surface. The reflectances were measured for angles of incidence of near normal, 20, 40, and 60 deg. It was found in all cases that the reflectance of the cryodeposit-substrate complex was quite different from that of the bare substrate. In particular, cryodeposits formed on a black surface increased the reflectance by a factor of from 10 to 20, depending on the angle of incidence, deposit thickness, and wavelength considered. The reflectance data obtained were used in a computer program to calculate the spectral distribution and total amount of 6000°K blackbody energy

reflected from cryodeposits. The total reflectance was computed for the wavelength range from 0.36 to 1.15 μ and allows a comparison with total reflectance measurements obtained earlier (Ref. 4).

SECTION II
TECHNIQUE OF REFLECTANCE MEASUREMENTS

The reflectance measurements were made using a vacuum integrating sphere. Normally, an integrating sphere is operated at atmospheric conditions. However, since the cryodeposits of interest are formed in a vacuum, the reflectance should be measured in situ to obtain meaningful results. Also, the vacuum reduces the gas impurity level and may affect the crystalline form of the deposit. No appreciable change in the reflectance of the magnesium oxide (MgO) coating was noted in going from atmospheric pressure down to 10^{-7} torr.

The monochromatic directional reflectance measured in the vacuum integrating sphere was obtained by the angular-hemispherical technique illustrated in Fig. 1. Radiation within a differential solid angle $\Delta\omega_i$ enters the sphere (Fig. 2) and is incident on the test surface at an angle ψ measured from the normal, N. The energy reflected strikes the MgO-coated hemisphere facing the test surface and is then reflected diffusely throughout the sphere. After multiple reflections within the sphere, the intensity at the wall is measured by a detector. The test surface is then rotated 180 deg so that the radiation entering the sphere is incident on the MgO coating on the back side of the test surface. The energy reflected from this MgO surface is similarly measured by the detector and is taken as a reference. For both sample and reference measurements, the detector does not view the first reflection. Using the two detector readings, B_S and B_{MgO}, the reflectance of the test surface, ρs, compared to the MgO surface reflectance, ρ_{MgO}, can be determined from the equation

$$\frac{\rho_s}{\rho_{MgO}} = \frac{B_s}{B_{MgO}} \tag{1}$$

From Eq. (1) it can be seen that the ratio of B_S to B_{MgO} gives the sample reflectance relative to the MgO reflectance. All reflectance results in this report are presented as relative measurements. However, the reflectance of MgO is near unity (from 0.95 to 0.98) over the wavelength range investigated, and hence the relative reflectance values can be interpreted as approximate absolute values.

SECTION III
APPARATUS

A schematic diagram and sketch of the integrating sphere system are shown in Figs. 2 and 3. The integrating sphere consisted of two flanged hemispheres which were vacuum sealed by an O-ring. They were coated internally with MgO approximately between 1 and 2 mm thick. The sphere has five entrance ports which account for about 3 percent of the total sphere surface area. These ports accommodate the vacuum pump, detector, cryosurface, incident radiation, and visual observation.

The pumping system consisted of an ion pump and a 4-in.-diam oil diffusion pump equipped with a LN_2-cooled cold cap and backed by a mechanical pump. The ion pump minimizes the possibility of oil backstreaming. The test cryosurface will also pump gases that will condense on a 77°K surface, but it was not used for pumpdown of the chamber. A thermocouple gage and an ionization gage were used to measure the pressure in the system.

The cryosurface was a hollow rectangular copper block of outside dimensions 1 by 1-1/2 by 2-1/2 in. and was cooled by circulating LN_2 through it. The LN_2 transfer line between the cryosurface and external LN_2 supply was vacuum jacketed to prevent cryodeposits from forming on it. One of the 1-1/2- by 2-1/2-in. sides of the cryosurface was used as a test surface. It was either coated with Cat-a-lac black paint or was just the bare polished copper surface. The reverse side of the cryosurface was coated with MgO approximately 2 mm thick and was used as the MgO reference surface. Since the cryosurface could be rotated through 270 deg, it was possible to illuminate either side. This also allowed reflectance measurements to be made as a function of angle of incidence of the light beam on the test surface. The test surface was irradiated with monochromatic light, using a tungsten-iodine (W-I) lamp and a prism monochromator. Radiation intensity on the sphere wall was detected by a photomultiplier tube having an S-1 response.

To control the test gas, H_2O or CO_2, entry into the chamber, a calibrated flow rate was required. The water (gaseous) addition system, shown in Fig. 4a, consisted primarily of a boiler, condenser, surge tank, and a rotameter (flowmeter). This system was first evacuated by means of a mechanical pump. The forepressure of the system was provided by the vapor pressure of the distilled water in the boiler. Water circulating through the condenser kept the distilled water in the

boiler at constant temperature. Also, the condenser prevented any liquid from going into the chamber, thereby ensuring a flow of only water vapor. The surge tank helped to maintain an essentially constant forepressure for the rotameter. This precaution was necessary since the calibration curve for the mass flow rate versus forepressure is nonlinear.

The CO_2 gas addition system was simpler than the H_2O system and is shown in Fig. 4b. In this system, a standard leak was used to introduce commercially pure CO_2 into the chamber. The leak rate was varied by using different standard leaks. For both CO_2 and H_2O gas addition systems, the mass flow rate was of the order of 10^{-3} gm/sec. The test gas entered the integrating sphere through the pump port (Fig. 3).

SECTION IV
PROCEDURE

Prior to each experiment, the interior of the integrating sphere was cleaned and recoated with MgO by burning magnesium ribbon below each hemisphere. In this way a freshly prepared MgO coating, from 1 to 2 mm thick, was always used. The cryosurface was also coated with MgO except for the face used for the test surface. Since these MgO coatings were very fragile, the system had to be pumped down gradually. The system pressure was slowly reduced by use of a mechanical pump. When the pressure was approximately 10 μ, the diffusion pump was started. After the pressure in the chamber had been reduced to 10^{-5} torr, the ion pump was started, and the diffusion pump valved off. Pumping continued until the pressure leveled off at about 10^{-7} torr, which usually required two or three days. With the system at equilibrium and the test surface at room temperature (300°K), reflectance measurements were made as a function of wavelength and angle of incidence. After completion of these measurements, the LN_2 flow was started and the test surface cooled to near 77°K. In some instances, the test surface reflectance was monitored during cooldown. After the surface temperature dropped to approximately 77°K the ion pump was shut off. The test gas was then admitted to the system and pumped by the cryosurface. After a specified time interval, the flow was stopped and the reflectance measurements were made. After completing these measurements, the flow of test gas into the system was resumed. This procedure was continued until a cryodeposit thickness of from 1 to 2 mm was obtained. Other investigations on cryodeposits have shown little effect, if any, because the deposits were formed in layers.

The pressure in the chamber during deposition varied from approximately 10 to 500 μ. This depended on the flow rate, the species of the test gas, and the thickness of the cryodeposit which had already been formed. The flow rates used for CO_2 were 2.4×10^{-3} and 2.6×10^{-4} gm/sec. Three flow rates were employed for water: 1.44×10^{-3}, 1.01×10^{-3}, and 0.82×10^{-3} gm/sec. For a given gas species and flow rate, the chamber pressure increased with deposit thickness, which indicates that there was a decrease in the capture coefficient for increasing deposit thickness. Each time before the reflectance measurements were made, the diffusion pump was used to pump out those gases in the chamber which had not condensed on the 77°K surface.

An approximate method was used to determine the cryodeposit thickness since this quantity was not directly measurable. The average thickness, ℓ_{av}, was calculated from the following equation

$$\ell_{av} = \frac{\dot{m}t}{A_c D} \tag{2}$$

where $\dot{m}$ is the mass flow rate of the test gas, t is the time of flow, A_c is the surface area of the cryosurface (94.6 cm^2), and D is the density of the cryodeposit. The thickness calculated represents an average thickness because of edge effects. Also, the density of the cryodeposit is not accurately known. For H_2O cryodeposits, the density was taken to be 0.9 gm/cm^3 (Ref. 5) whereas, for CO_2 cryodeposit, a density of 1.5 gm/cm^3 (Refs. 5 and 6) was used. Actually, the cryodeposit density is probably variable because of the many crystalline forms possible for H_2O and CO_2 frosts. The crystalline forms may depend on the test gas flow rate, the pressure in the chamber during deposition, and the local cryodeposit thickness.

SECTION V
RESULTS AND DISCUSSION

5.1 EXPERIMENTAL RESULTS

5.1.1 H_2O Cryodeposits

The reflectance for H_2O cryodeposits formed on a Cat-a-lac black painted surface is shown in Figs. 5 through 8. A flow rate of 1.01×10^{-3} gm/sec water vapor was used for these experiments. Figures 5 through 8 are for angles of incidence of 0, 20, 40, and 60 deg, respectively. In these and subsequent figures, some curves are labeled 77°K (ℓ_{av} = 0.0 mm) and/or 300°K (ℓ_{av} = 0.0 mm). These are the spectral reflectance curves

for the test surface at the designated temperature prior to admitting any test gas to the chamber. It should be noted that even though ℓ_{av} = 0.0 mm is designated on the 77°K curves there is a very thin cryodeposit film present on the test surface caused by cryopumping of residual gases in the system. Reflectance measurements are shown for cryodeposit thicknesses of 0.11, 0.22, 0.33, 0.44, 0.88, and 1.32 mm. As observed previously for CO_2 (Ref. 7), the reflectance at shorter wavelengths increases most rapidly with deposit thickness until a thickness of approximately 0.25 mm is attained. When the cryodeposit thickness increases further, the spectral reflectance curve begins to flatten out and reaches a plateau near 100 percent depending on the wavelength and angle of incidence. (Note: These measurements are relative to the reflectance of MgO.) The sharp increase in reflectance at the shorter wavelengths (for small thicknesses) indicates that some form of wavelength-dependent scattering is occurring. As the deposit thickness increases, internal scattering becomes the predominant factor.

Reflectance measurements were also made for H_2O cryodeposits formed at other flow rates on both Cat-a-lac black and polished copper. The reflectance for H_2O deposits formed on Cat-a-lac black at the flow rate of 1.44×10^{-3} gm/sec is presented in Fig. 9. These reflectance curves are quite different from the previous ones. Most noticeable is the strong absorption region which occurs in the wavelength range from 0.8 to 1.1 μ. This difference is thought to be caused by the larger flow rate resulting in the deposit being formed at higher pressure. As can be seen from Fig. 10, this strong absorption region was also observed for H_2O deposits formed on a polished copper substrate. The flow rate used in forming these deposits was again 1.44×10^{-3} gm/sec. It is noted from Fig. 10 that the reflectance of copper varies considerably with wavelength in the visible and near infrared. At the short wavelengths, the reflectance is low, but it increases sharply at approximately 0.55 μ and attains a high value at the longer wavelengths. It was observed that the presence of water cryodeposit on copper increased the reflectance at short wavelengths but greatly reduced the reflectance in the range from 0.8 to 1.1 μ.

In Fig. 11, the reflectance is presented for an H_2O deposit formed on polished copper at a flow rate of 0.82 gm/sec which is less than the flow rate of Fig. 10 (1.44×10^{-3} gm/sec). Similar to the results of Figs. 5 through 8, no strong absorption region was observed for the cryodeposits formed at this low flow rate. It is noted in Fig. 11 that the spectral reflectance of the bare polished copper is substantially less than the value presented earlier in Fig. 10. This is because the copper surface was not as highly polished for the latter set of experiments. It

is also observed in Fig. 11 that for a deposit thickness of 0.77 mm the reflectance is substantially increased at all wavelengths. However, the greatest increase still occurs in the short wavelength region.

The difference in the two types of reflectance curves obtained for H_2O cryodeposits can probably be attributed to the size of the particles or crystals formed at the two different flow rates or chamber pressures. Dunkle and Bevans (Ref. 8) predicted a similar phenomenon for the spectral reflectance of snow cover. Their theoretical results indicated an increase in absorption for increasing particle sizes with most of the absorption occurring in the wavelength range from 0.8 to 1.1 μ. In the present study, different crystalline forms were visually observed for cryodeposits formed under similar experimental conditions. Most of the deposits were much like a white frost. However, in one experiment the deposit formed in two distinctly different layers even though the flow rate was held constant throughout at 0.82×10^{-3} gm/sec. One layer (the outer) had the usual white frost appearance while the other layer (the inner) was composed of small transparent crystals. For this particular cryodeposit, the reflectance (Fig. 12) did not increase rapidly with thickness. At a thickness of 1.17 mm, the reflectance was still below 40 percent, and the large reflectance increase only began when the deposit started forming like white frost. In general, the reflectance of the H_2O deposits varied considerably from one experiment to the next, and duplication of any one deposit was difficult.

5.1.2 CO_2 Cryodeposits

The spectral reflectance CO_2 cryodeposits on a Cat-a-lac black substrate was previously measured over the visible wavelength range (Ref. 7). In the present study, these spectral measurements were extended out to a wavelength of 1.15 μ and both Cat-a-lac black and polished copper substrates were employed. The spectral reflectance of a CO_2 deposit on Cat-a-lac black is presented in Figs. 13 through 16 for angles of incidence of 0, 20, 40, and 60 deg, respectively. The general shapes of the reflectance curves for CO_2 cryodeposits are very similar to those obtained for the H_2O cryodeposits when no strong absorption regions were present (Figs. 5 through 8). It is also seen that, similar to the results for H_2O, the presence of a CO_2 cryodeposit on a Cat-a-lac black surface increases the reflectance greatly. For example, in Fig. 13 the reflectance with a thick (1.83-mm) deposit present ranges from approximately 75 down to 60 percent. It should be noted, however, that, for a given deposit thickness and angle of incidence, the reflectance of a CO_2 cryodeposit (Figs. 13 through 16) is substantially less than that of H_2O cryodeposits (Figs. 5 through 8).

In Fig. 17, the spectral reflectance of a CO_2 deposit on polished copper is presented for an angle of incidence of 20 deg. It is noted that even for thick deposits the effect of the copper substrate reflectance is still present at wavelengths greater than about 0.55 μ.

In general, it was found that the CO_2 deposit reflectance increased more with angle of incidence than did the H_2O deposit reflectance. This would imply that H_2O deposits reflect more diffusely than do CO_2 deposits. However, some of the CO_2 deposits were observed to have directionally oriented "pinholes." It was possible to see the substrate through these pinholes even though the deposit was as much as 2 mm thick. No such pinholes were observed in the H_2O deposits. This difference in the structure of the CO_2 and H_2O cryodeposits could partially explain the greater dependence of the CO_2 reflectance on angle of incidence. Thus, the reflectance of the CO_2 deposits may be determined not only by the absorption and scattering properties of the CO_2 frost but by the geometrical formation properties as well.

5.2 REFLECTANCE MEASUREMENTS OF THIN CRYODEPOSIT FILMS

It is noted in Fig. 9 that the reflectance was measured for an H_2O cryodeposit which was only 0.020 mm (20 μ) thick. For this cryodeposit thickness, the reflectance is about one-half that of the bare Cat-a-lac black surface. Over most of the wavelength range the reflectance is reduced from approximately 4.0 down to 2.0 percent. A similar reduction in reflectance was observed during cooldown of the cryosurface. This phenomenon occurred even though no test gas was introduced into the system. An illustration of this effect is shown in Fig. 18 where the reflectance is plotted as a function of the time after initiation of LN_2 flow through the cryosurface. These results were obtained using incident radiation of 0.52-μ wavelength. The same effect was also observed for a polished copper substrate. This reduction in reflectance is produced by a very thin film of H_2O or CO_2 cryodeposit which forms on the test surface. These cryodeposits are formed from residual gases which are still present in the chamber at a pressure of 10^{-7} torr. This reflectance reduction effect is similar to the "lens coating" effect (Ref. 9) where a film of thickness $\lambda/4n$ is deposited on the surface of a lens to reduce reflection losses. In the relation $\lambda/4n$, λ is the wavelength of the incident radiation and n is the refractive index of the film.

In Fig. 19, a vivid illustration is given of how thin cryodeposit films affect the surface reflectance. These results were obtained by monitoring the reflectance of a polished copper cryosurface as a function of time. As noted, the reflectance of the surface prior to cooldown was 45 percent.

Both during and after cooldown the surface cryopumped residual gases that were still present in the chamber. Thus, a very thin cryodeposit formed on the polished copper surface and this caused the reflectance to decrease to approximately 36 percent. When the test gas (CO_2) flow was started (t = 0), the reflectance immediately went through a series of successive minima and maxima as shown. Since test gas flow time determines deposit thickness, the resulting curve for $t \geq 0$ can be interpreted as the variation of reflectance with cryodeposit thickness. A thickness scale determined from Eq. (2) is also given on the figure. This particular reflectance variation was obtained using near-normal incident radiation of 0.52-μ wavelength. The angle of incidence was 5 deg since for normal incidence the radiation would be reflected back through the entrance port. Similar reflectance patterns were observed for other angles of incidence and other wavelengths and also for H_2O deposits on both Cat-a-lac black and copper substrates.

The reflectance patterns observed in Fig. 19 result from interference phenomena which are generated by the presence of thin cryodeposits on the substrate surface. When the interference between reflected light rays is destructive, minima are observed in the reflectance curve (Refs. 9 and 10). For any particular angle of incidence, the film thicknesses corresponding to these reflectance minima are given by the relation

$$d = \frac{(m + 1/2)\lambda}{2n \cos \theta'} \tag{3}$$

where d is the thickness, m = 0, 1, 2, . . . is the order of the interference, and θ' is the angle of refraction. If the interference between reflected light rays is constructive, maxima are observed in the reflectance curve. The film thicknesses corresponding to these reflectance maxima are given by the expression

$$d = \frac{m\lambda}{2n \cos \theta'} \tag{4}$$

Equations (3) and (4) were derived under the assumption that the refractive index of the deposit layer is less than that of the substrate. It was also assumed that the phase shift is 180 deg when radiation is reflected on passing from a low refractive index region to a higher one.

From the equation of the reflectance minima, it is shown that for normal incidence the deposit thickness may be determined from the relation

$$d = \frac{(2m + 1)\lambda}{4n} \tag{5}$$

Thus, by knowing refractive index of the deposit, it is possible to utilize this interference phenomenon for in situ optical thickness measurements of thin cryodeposit films. Efforts are currently being made to determine the refractive index and in situ thicknesses of CO_2 cryodeposits.

5.3 COMPUTER RESULTS

Once the spectral reflectance of cryodeposits has been measured over the wavelength range from 0.36 to 1.15 μ, the reflected solar energy may be determined for the same wavelength range. This result can be used as a quantitative estimate of the solar radiation reflected from cryodeposits on space chamber walls. With this in mind, a computer program was written to calculate the total cryodeposit reflectance for incident solar radiation from 0.36- to 1.15-μ wavelength. The spectral energy distribution used for the solar irradiation was that of a 6000°K blackbody emitter. In setting up the numerical calculation procedure, the wavelength range from 0.36 to 1.15 μ was divided into approximately 35 intervals. These intervals were determined by adjacent points on the cryodeposit reflectance curve. In each interval, an average reflectance was determined. Using the technique described in Appendix II, the incident energy in each wavelength interval was computed from the energy distribution of a 6000°K blackbody. The energy reflected in each interval was found from the product of the average reflectance and the incident energy. The total energy reflected was found by summing up the reflected energy for all wavelength intervals. This value of the total reflected energy divided by the total incident energy in the wavelength range from 0.36 to 1.15 μ gives the total reflectance of solar radiation in the visible and near-infrared regions. Wavelength distribution curves are shown in Fig. 20 for the reflected radiation from H_2O and CO_2 cryodeposits 1.83 mm thick formed on a Cat-a-lac black substrate. These curves were calculated considering a 6000°K blackbody as the source and using the spectral reflectance measurements for normal incidence (ψ = 0 deg) radiation.

The computer program was used for obtaining the total reflectance of both H_2O and CO_2 cryodeposits formed on a Cat-a-lac black substrate. In both cases, the angle of incidence of the radiation was 0 deg (normal to the surface). For a 1.83-mm H_2O deposit with significant absorption, the calculated total reflectance was 80 percent. The spectral reflectance of this particular deposit, but for an angle of incidence of 20 deg, is shown in Fig. 9. For a CO_2 deposit of 1.83 mm, the calculated total reflectance was 67 percent. The spectral reflectance for this deposit is shown in Fig. 13. When the calculated value for the total reflectance of CO_2 deposit is compared with the experimental value of the total reflectance as measured in Ref. 4 (approximately 68 percent), the two values are approximately the same, even though the two methods should not be expected to yield the same values.

In addition to the calculated total reflectance of cryodeposits, the computer results also indicated that 9 percent of the radiant energy flux from a 6000°K blackbody is of wavelengths less than 0.36 μ, 71 percent is in the wavelength range from 0.36 to 1.15 μ, and 20 percent is of wavelengths greater than 1.15 μ.

SECTION VI
PLANETARY ENVIRONMENT STUDIES

The radiative properties of frosts are of interest in regard to the planetary atmospheres of Mars and Venus. Recently, Leighton and Murray (Ref. 1) proposed a thermal model of the Martian surface which correlated the surface pressure and temperature with the radiative properties of the Martian soil and polar caps. In this model, the solar reflectances of the soil and polar caps were assumed to be 0.15 and 0.65, respectively. The authors stated that they were not aware of any published solar reflectance data for CO_2 and H_2O frosts formed under simulated Martian conditions. After viewing this statement, the environmental conditions used in the present experiments were compared with current estimates of the environmental conditions on Mars. This comparison led to the conclusion that the formation of CO_2 and H_2O frosts on the Cat-a-lac black surface in the present experiments approximates the formation of CO_2 and H_2O frosts on the Martian surface. In both cases, the deposits are formed on a poor reflector at low pressures. The pressure on Mars is thought to be between 5 and 10 mb depending on the time of the year (Ref. 11). In the present experiments, the deposits were formed at pressures ranging from 0.1 to 0.5 mb and, as mentioned previously, the deposit formation may depend on the surrounding pressure. As noted in Fig. 13 for near-normal irradiation, the reflectance of thick (1.83-mm) CO_2 frost on Cat-a-lac black decreases from about 75 percent at the shorter wavelengths to 60 percent at the longer wavelengths. For thick H_2O frosts formed at the higher flow rates on a Cat-a-lac black surface (Fig. 9) the reflectance (relative to MgO) is from 90 to 100 percent except in the wavelength region where the absorption band occurs.

In the previously mentioned article by Leighton and Murray, it was also pointed out that the reflectance of CO_2 frost may depend on the irradiation incidence angle. However, the reflectance values used in that investigation were for normal irradiation. In the present experiments for CO_2, it was found that for a deposit 1.83 mm thick the reflectance for irradiation at an angle of 60 deg was at least 15 percent greater than for near-normal irradiation.

Keegan and Weidner (Ref. 2) have also investigated frost reflectances for "fingerprinting" the clouds of Venus. Their measurements were made on various types of frosts which were formed at atmospheric pressure. These measurements were made for wavelengths between 2.5 and 20 μ, and in so doing, the absorption bands and characteristic spectra in the infrared were obtained. The results obtained in the present investigation for the visible and near-infrared region could be used as a supplement to the infrared measurements. Strong (Ref. 3) compared the data of Keegan and Weidner with data obtained from balloon-telescope flights made in 1964. He concluded that the clouds of Venus were composed of ice crystals. Assuming Strong's conclusion to be correct, then any reflectance data which he may have obtained in the 0.8- to 1.2-μ region might exhibit the considerable absorption which was observed in some of the present experiments on the H_2O frosts.

SECTION VII
CONCLUSIONS

From the results presented for the radiative properties of H_2O and CO_2 cryodeposits formed on Cat-a-lac black paint and polished copper surfaces, the following conclusions can be made for wavelengths between 0.36 and 1.15 μ.

1. For either an H_2O or CO_2 cryodeposit thickness of from 1 to 2 mm, the spectral reflectance of a black painted surface will be increased by a factor of from 15 to 20.
2. In general, for the same deposit thickness, the reflectance of the H_2O cryodeposit will be greater than that of the CO_2 deposit.
3. For near-normal incidence, the reflectance of an H_2O deposit on Cat-a-lac black reaches a plateau of from 85 to 100 percent (relative to MgO). For CO_2 this reflectance plateau is from 65 to 75 percent. The calculated deposit thickness at which this plateau occurs is between 1.0 and 2.0 mm.
4. The CO_2 deposit reflectance is more dependent on the angle of incidence than is the reflectance of the H_2O deposit.
5. For H_2O deposits formed at high flow rates, strong absorption was observed in the wavelength region from 0.8 to 1.1 μ. This effect may be caused by the deposit being formed at a higher chamber pressure, which results in different crystalline formations.

6. Using the computer program, the total reflectance was calculated for an H_2O cryodeposit which had a strong absorption region. The total reflectance for $0.36 < \lambda < 1.15\ \mu$ was found to be 80 percent. Similarly, the CO_2 deposit was found to have a total reflectance of 67 percent. Seventy-one percent of the radiant energy flux emitted from a 6000°K blackbody is within this wavelength range.

7. The CO_2 and H_2O frost reflectances measured in the present experiments may be useful in planetary environment studies.

8. The reflectance of Cat-a-lac black and copper substrates will exhibit interference patterns for thin films of cryodeposit. It may be possible to utilize this phenomenon for in situ optical thickness measurement of thin cryodeposit films.

REFERENCES

1. Leighton, Robert B. and Murray, Bruce C. "Behavior of Carbon Dioxide and Other Volatiles on Mars." Science, Vol. 153, No. 3732, July 1966, p. 136.

2. Keegan, H. J. and Weidner, V. R. "Frost Is Fingerprinted." U. S. Dept. of Commerce, Technical News, October 1965.

3. Bottema, Murk, Plummer, William, Strong, John, and Zander, Rodolphe. "The Composition of the Venus Clouds and Implications for Model Atmospheres." Journal of Geophysical Research, Vol. 70, No. 17, September 1965, p. 4401.

4. McCullough, B. A., et al. "Thermal Radiative Properties of Carbon Dioxide Cryodeposits from 0.5 to 1.1 Microns." AEDC-TR-65-94 (AD468632), August 1965.

5. Handbook of Chemistry and Physics, Chemical Rubber Publishing Co., 39th Edition, 1958, p. 535.

6. Caren, R. P., et al. "Experimental and Analytical Investigation of the Effect of Cryodeposits on the Radiation Properties of Plain and Extended Surfaces." AEDC-TDR-63-270 (AD425490), December 1963.

7. Wood, B. E., et al. "Vacuum Integrating Spheres for Measuring Cryodeposit Reflectances from 0.35 to 5 Microns." AEDC-TR-65-178 (AD468608), August 1965.

8. Dunkle, R. V. and Bevans, J. T. "An Approximate Analysis of the Solar Reflectance and Transmittance of a Snow Cover." Journal of Meteorology, Vol. 13, No. 121, 1956.

9. Clark, J. A., Ed. Theory and Fundamental Research in Heat Transfer. Pergamon Press, 1963, p. 16.

10. Jenkins, Francis A. and White, Harvey E. Fundamentals of Optics. McGraw-Hill Book Company, Inc., 1957, pp. 261-270.

11. Gross, S. H., McGovern, W. E., and Rasad, S. I. "Mars: Upper Atmosphere." Science, Vol. 151, March 1966, p. 1216.

12. Jackson, H. Tracy, Jr. and Ross, Richard J. "Planck's Radiation Equation Integrated." U. S. Army Missile Command, Redstone Arsenal, Alabama, RN-TR-66-1, January 1966.

APPENDIXES

I. ILLUSTRATIONS

II. METHODS OF CALCULATION

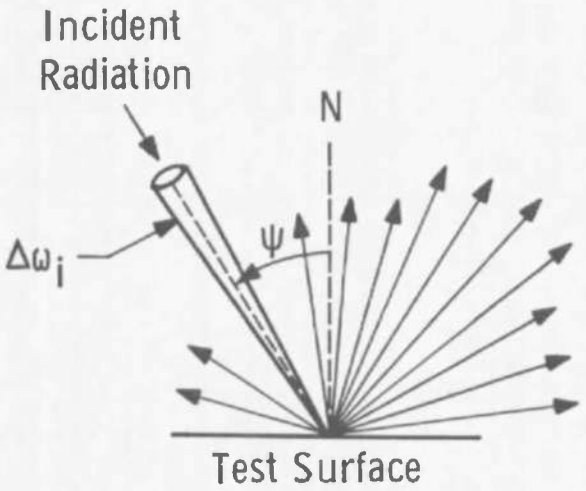

Fig. 1 Angular-Hemispherical Technique

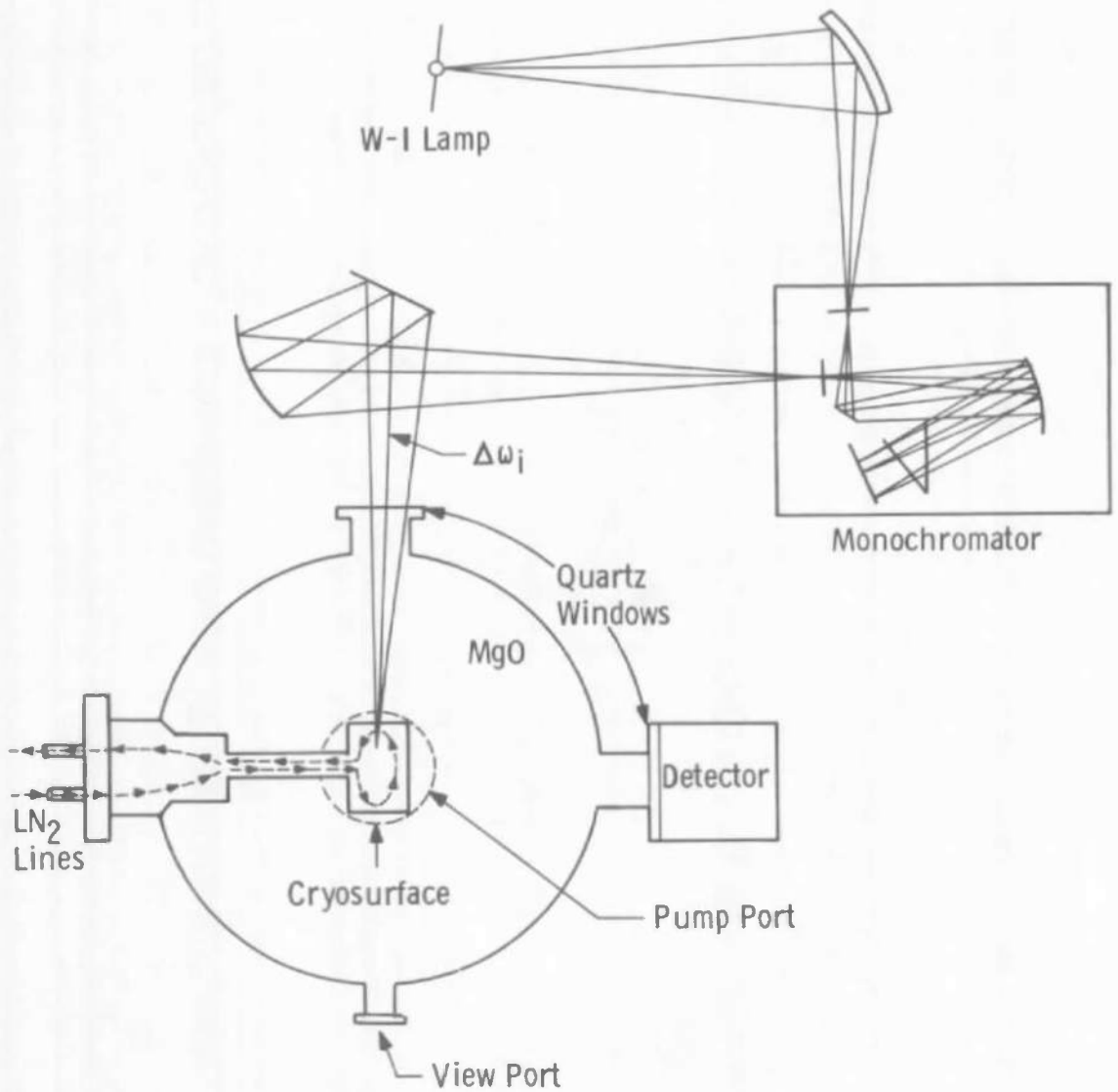

Fig. 2 Twelve-Inch Integrating Sphere System

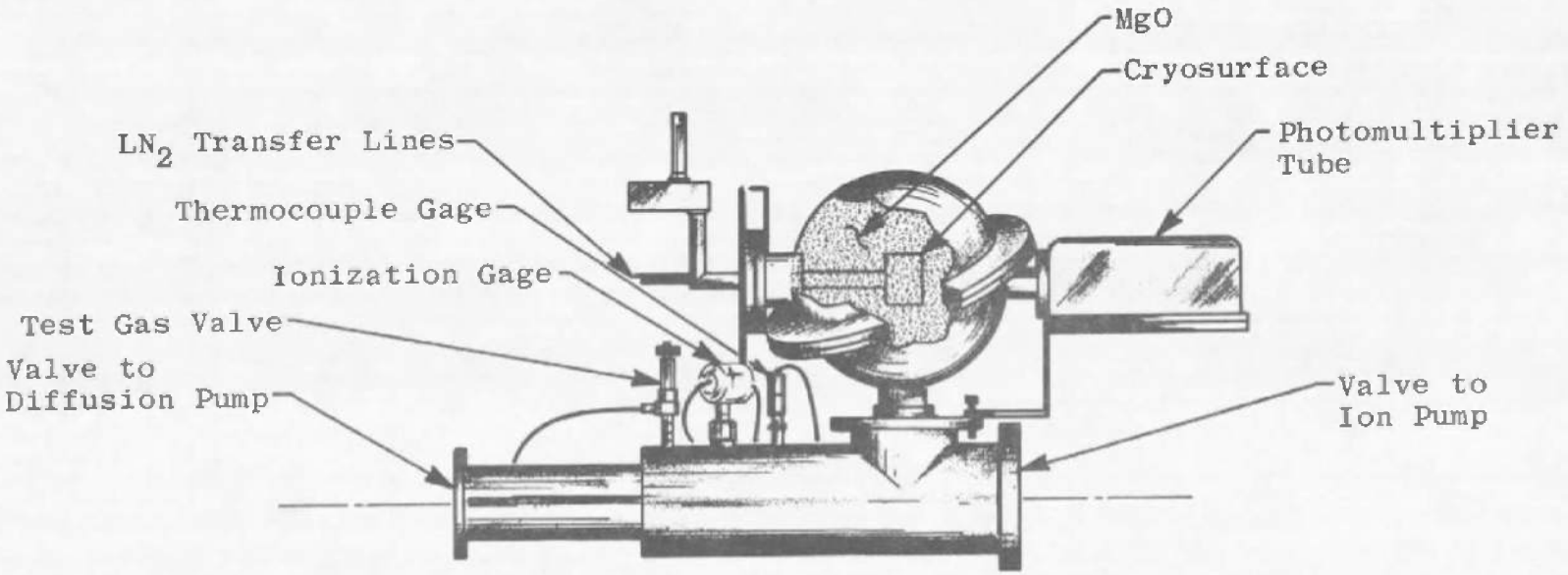

Fig. 3 Integrating Sphere and Pumping System

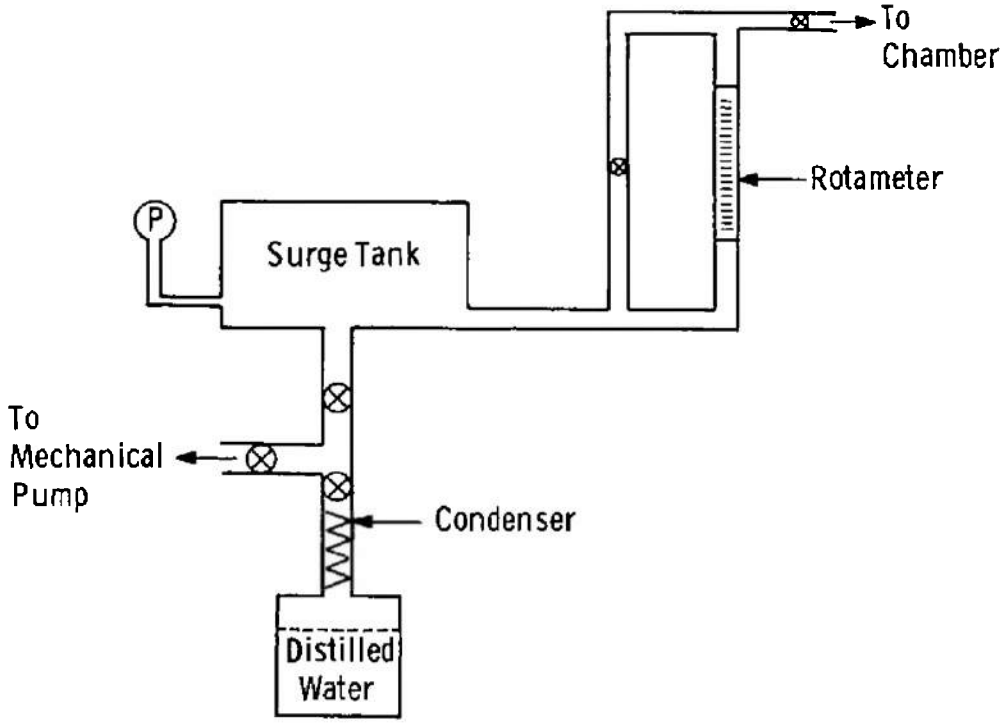

a. Water Addition System

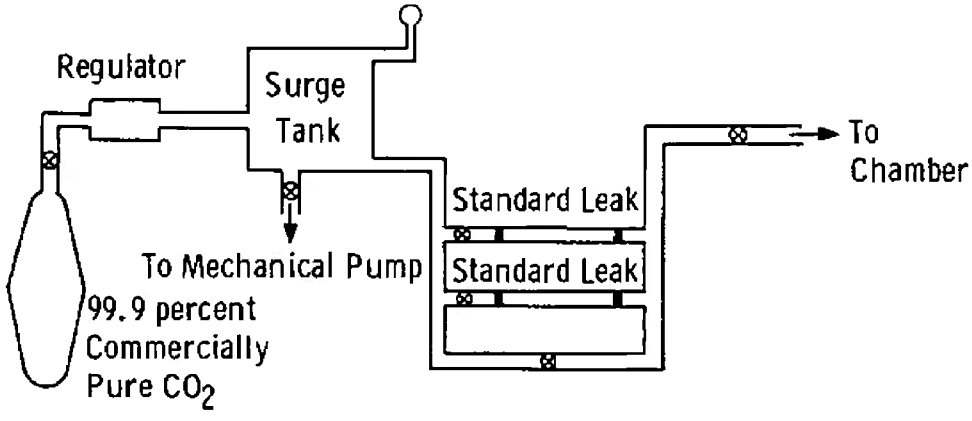

b. Carbon Dioxide System

Fig. 4 Gas Addition Systems

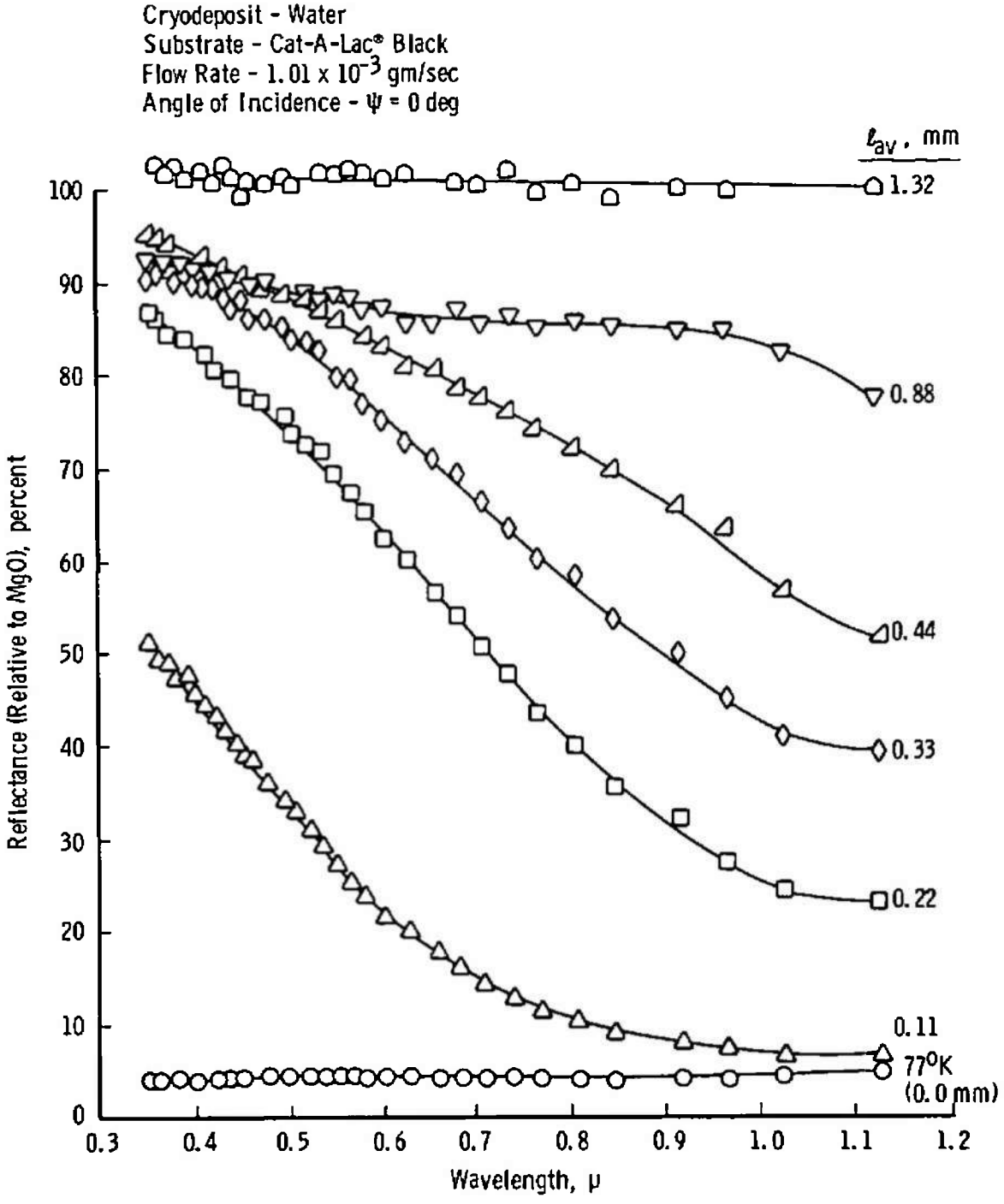

Fig. 5 Reflectance of Water Cryodeposits on Cat-a-lac Black, ψ = 0 deg

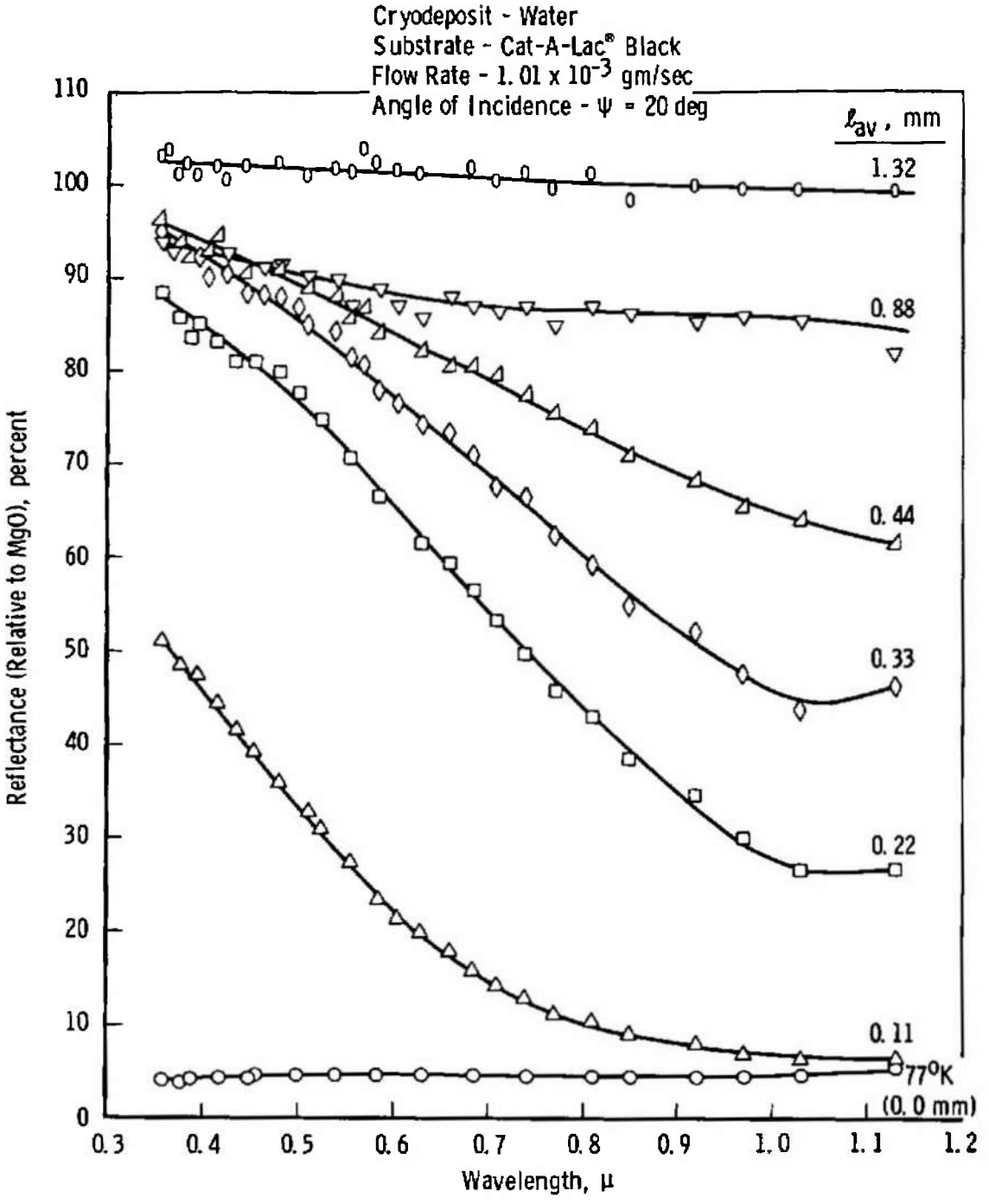

Fig. 6 Reflectance of Water Cryodeposits on Cat-a-lac Black, ψ = 20 deg

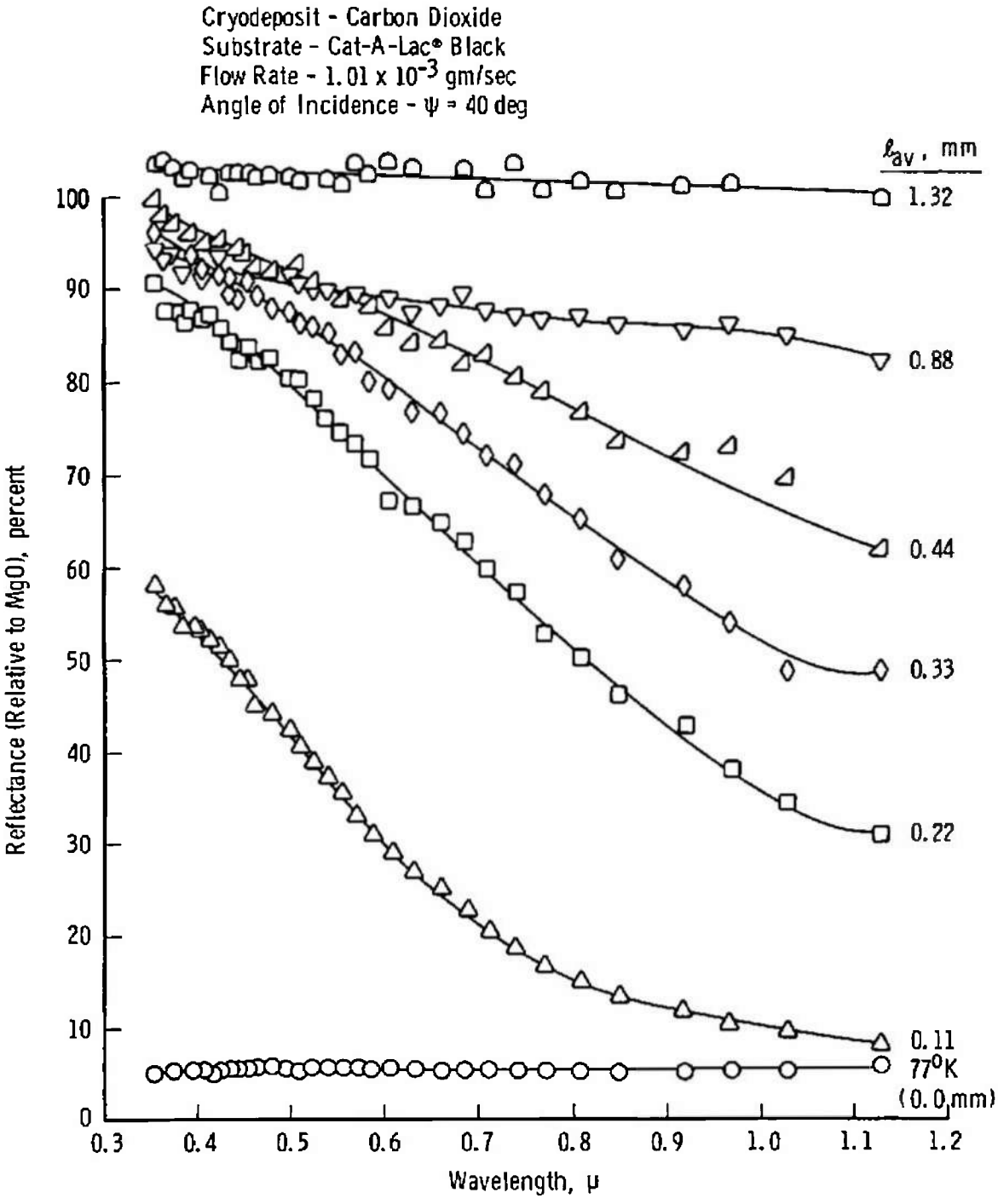

Fig. 7 Reflectance of Water Cryodeposits on Cat-a-lac Black, ψ = 40 deg

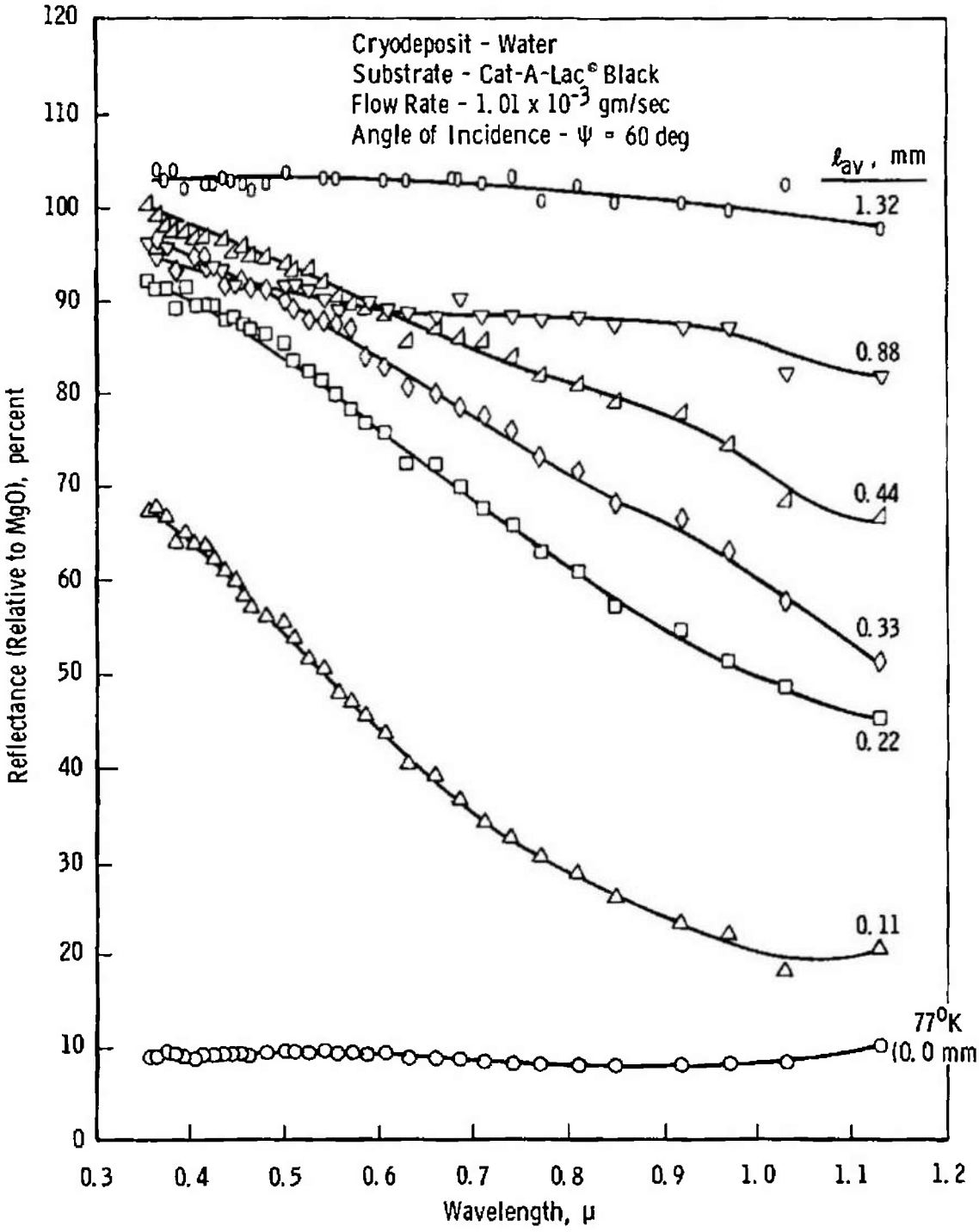

Fig. 8 Reflectance of Water Cryodeposits on Cat-a-lac Black, ψ = 60 deg

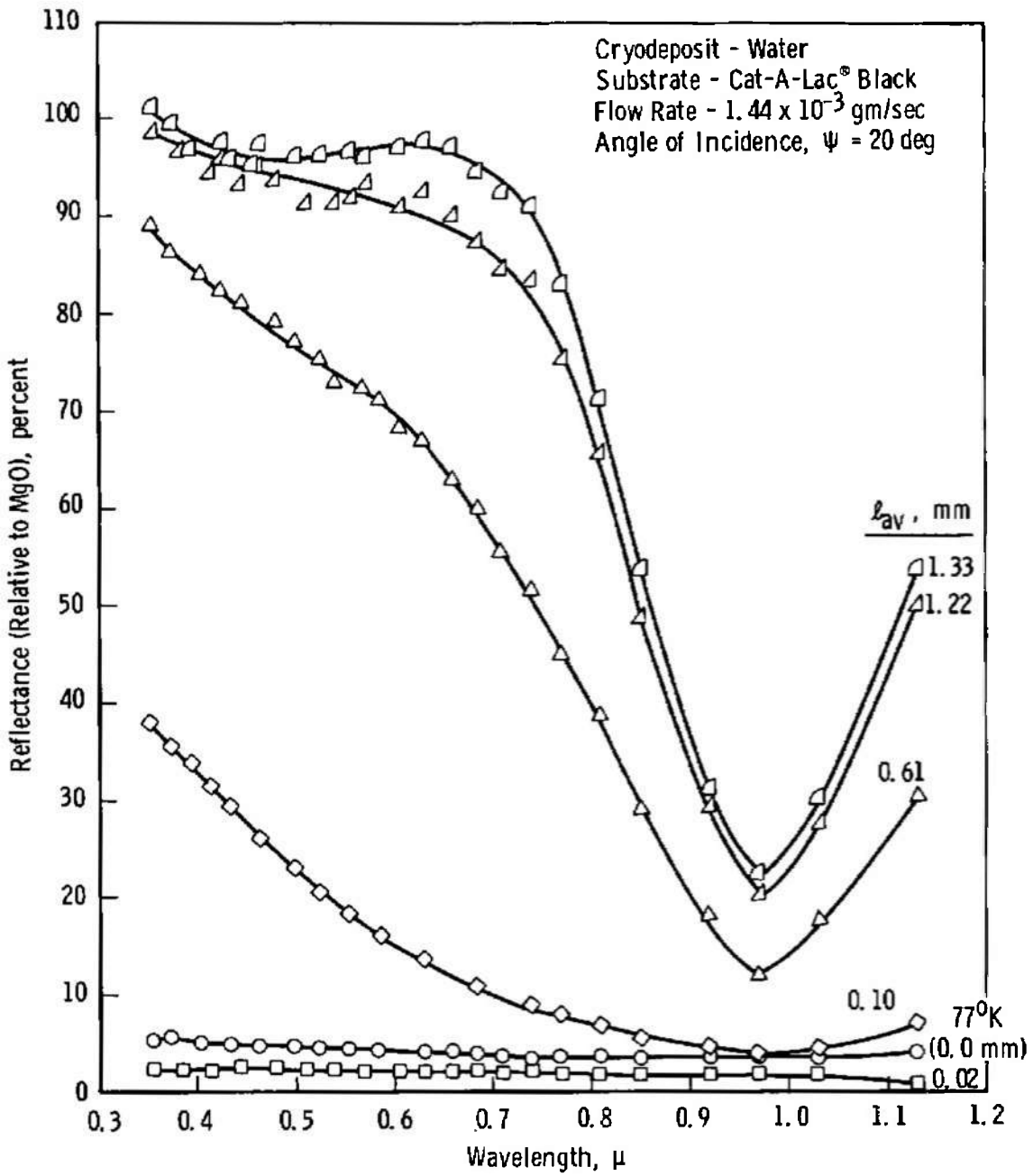

Fig. 9 Reflectance of Water Cryodeposits on Cat-a-lac Black, with Absorption, ψ = 20 deg

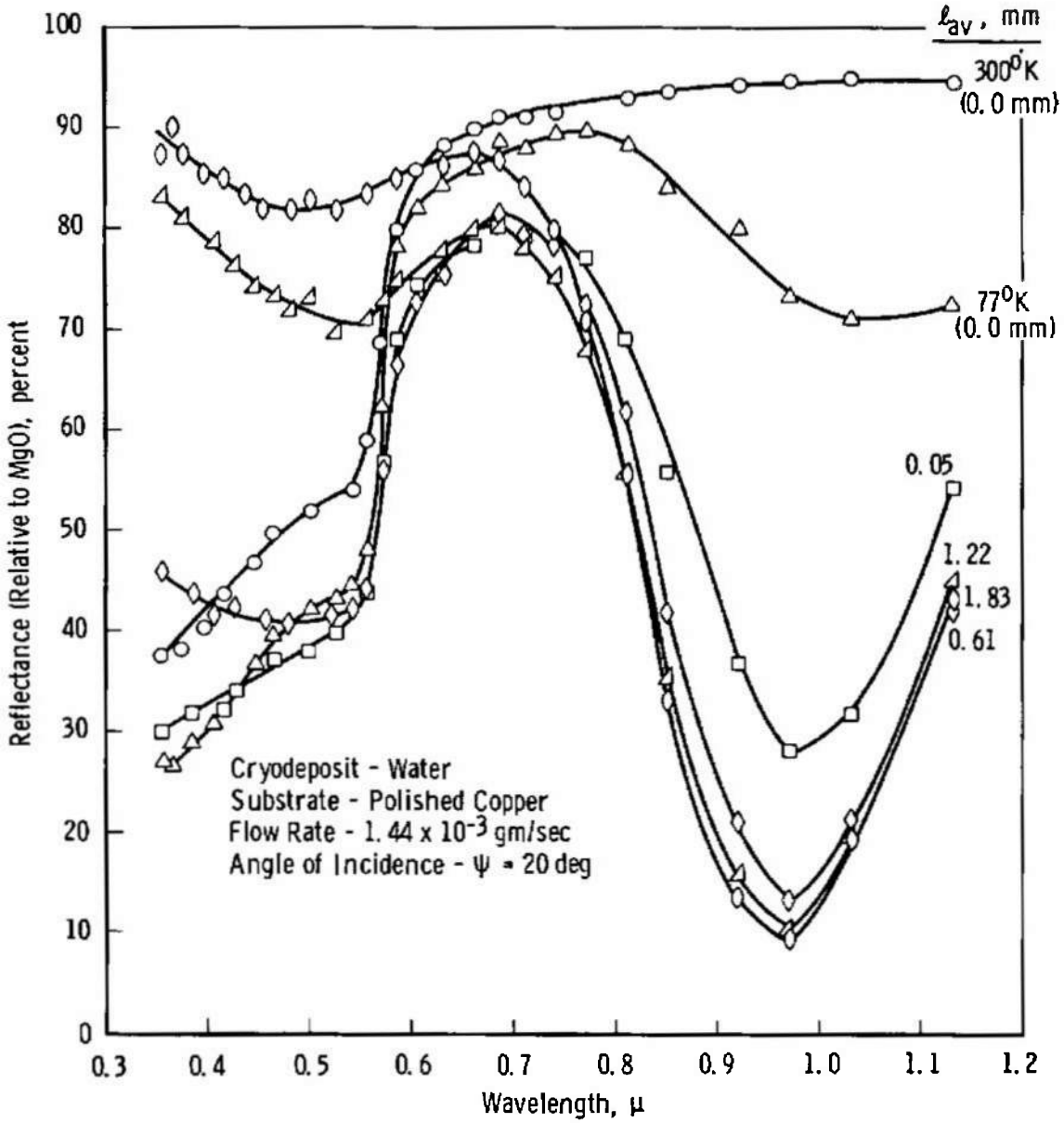

Fig. 10 Reflectance of Water Cryodeposits on a Copper Substrate, with Absorption, ψ = 20 deg

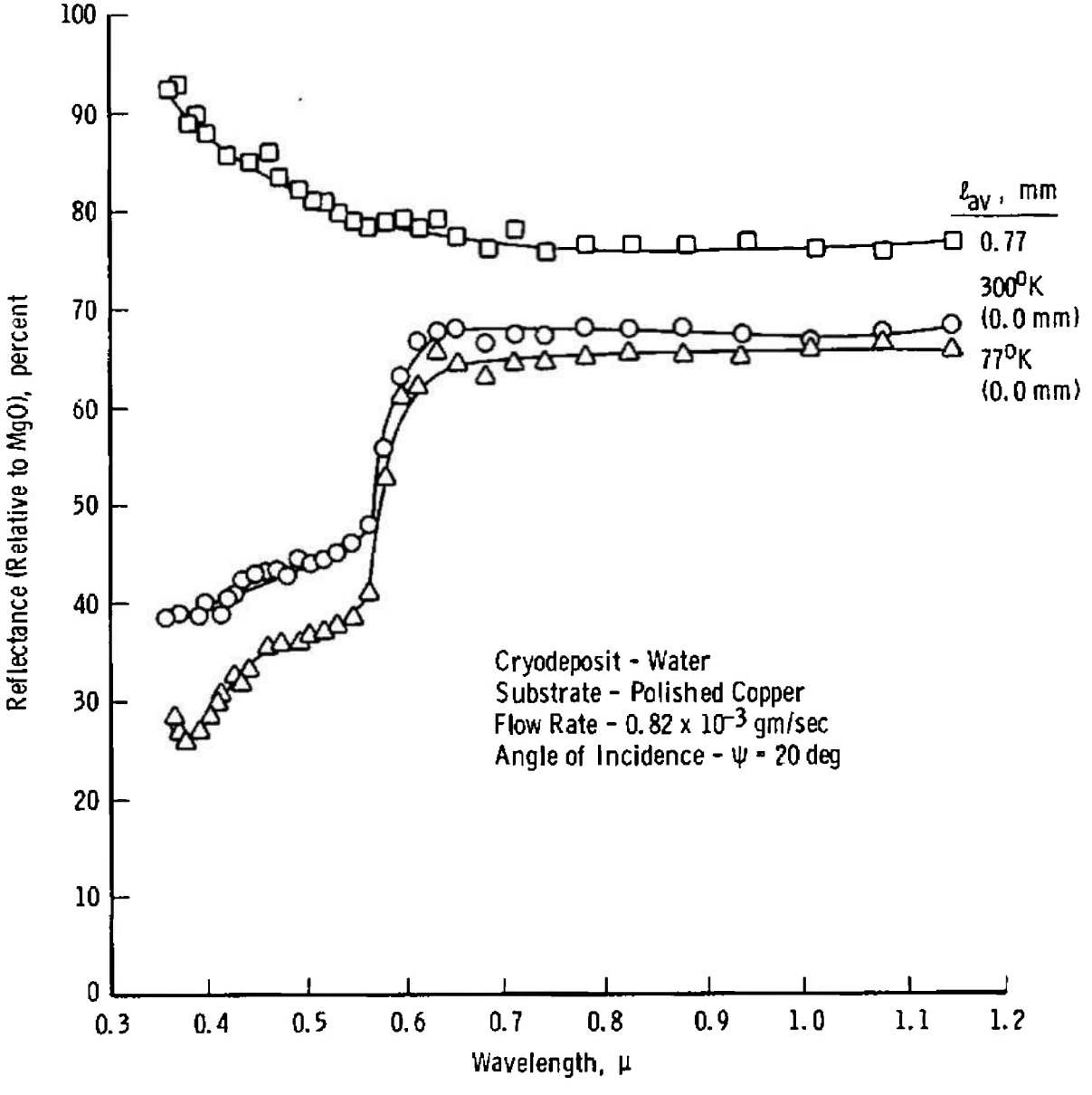

Fig. 11 Reflectance of Water Cryodeposits on a Copper Substrate, no Absorption, ψ = 20 deg

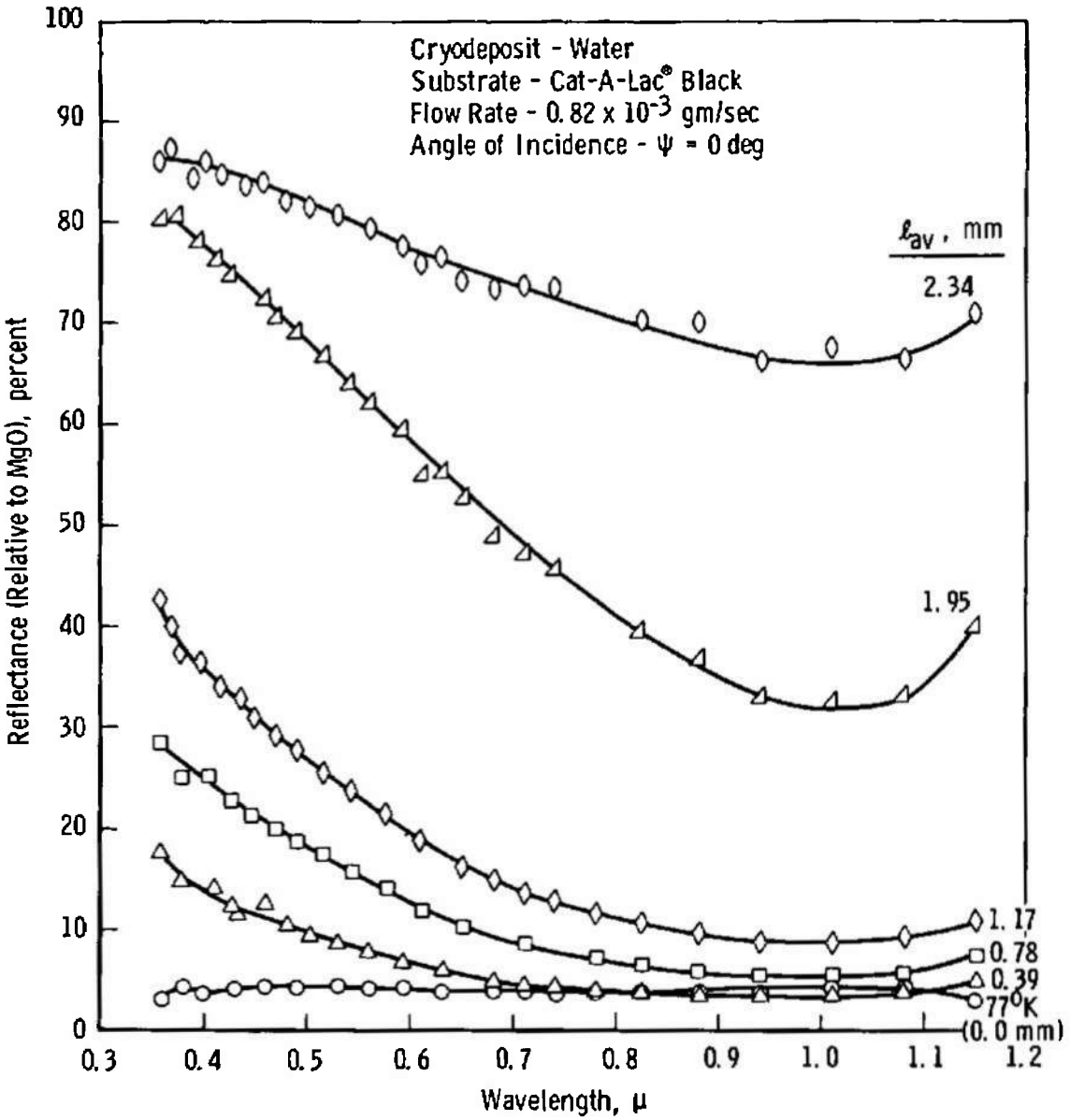

Fig. 12 Reflectance of Water Cryodeposits on Cat-a-lac Black, Weak Absorption, ψ = 0 deg

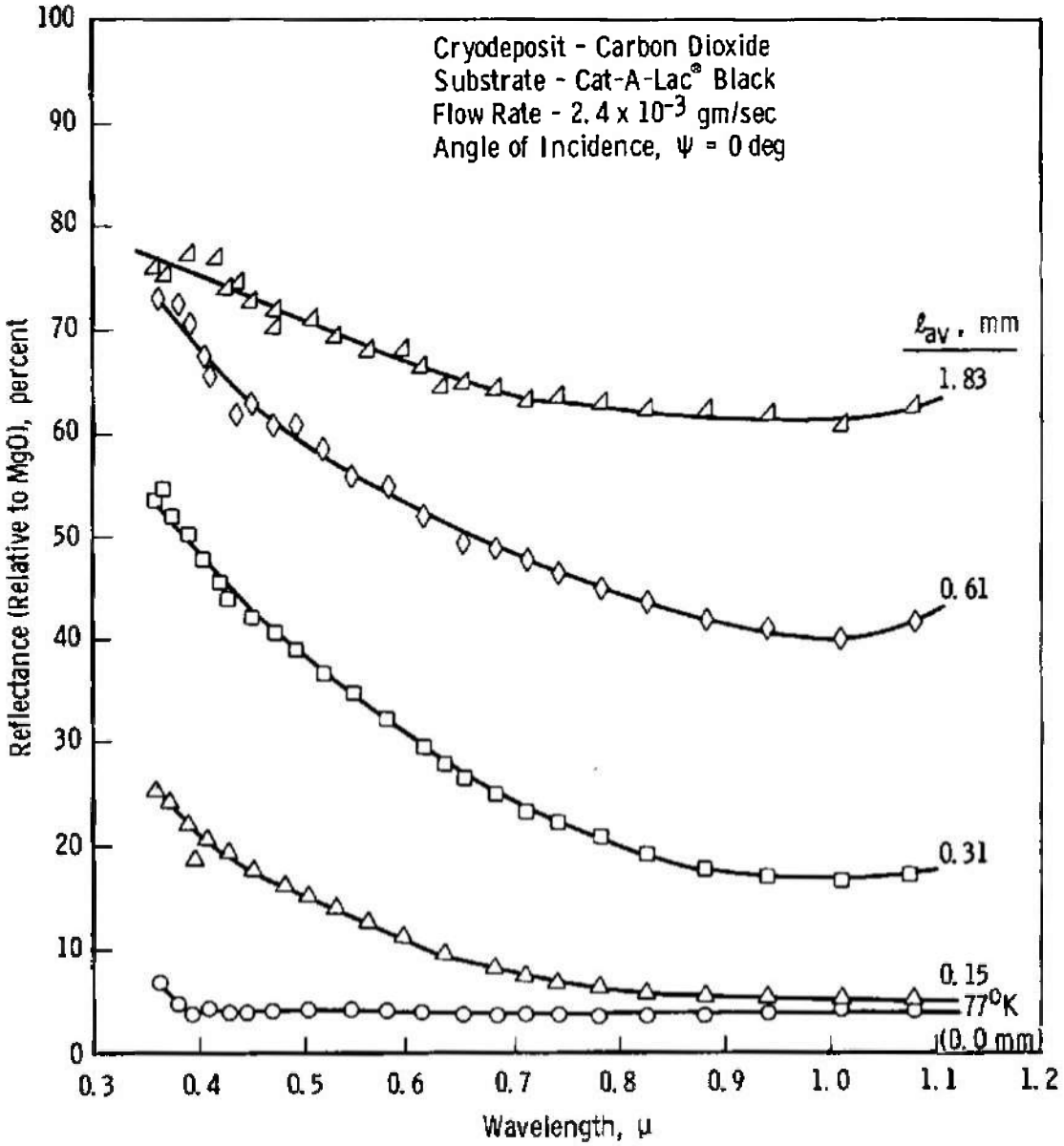

Fig. 13 Reflectance of Carbon Dioxide Cryodeposits on Cat-a-lac Black, ψ = 0 deg

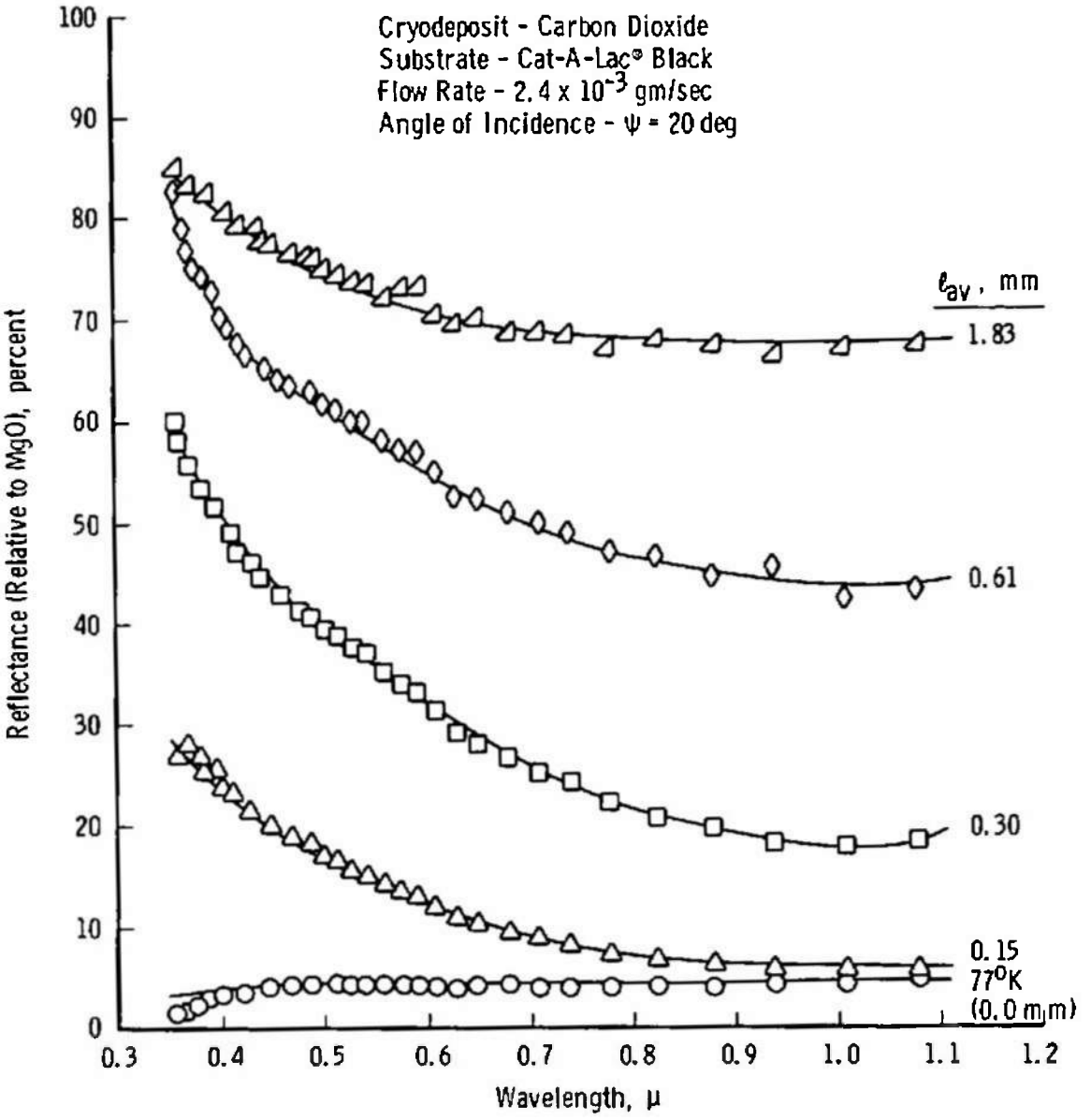

Fig. 14 Reflectance of Carbon Dioxide Cryodeposits on Cat-a-lac Black, ψ = 20 deg

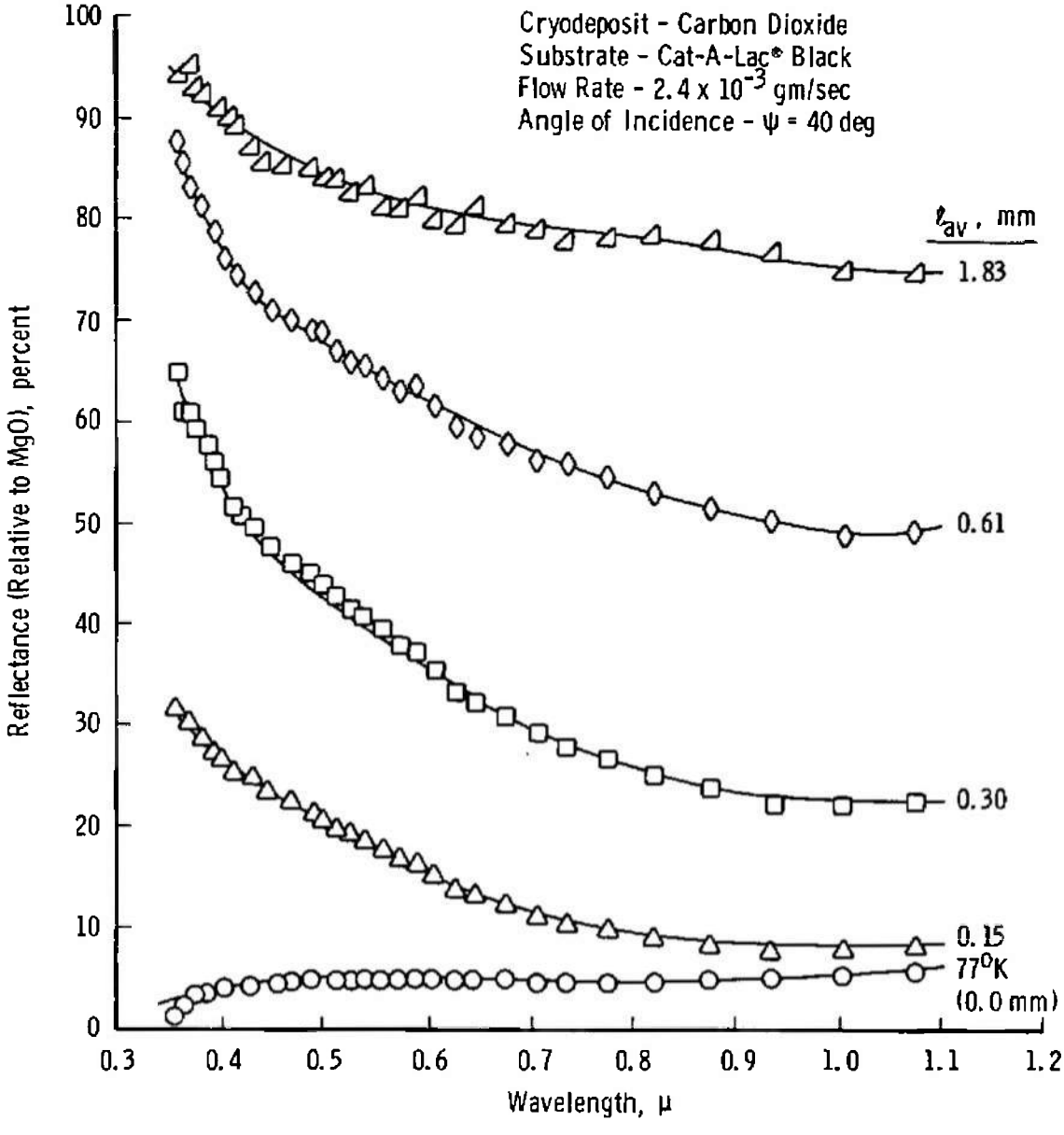

Fig. 15 Reflectance of Carbon Dioxide Cryodeposits on Cat-a-lac Black, ψ = 40 deg

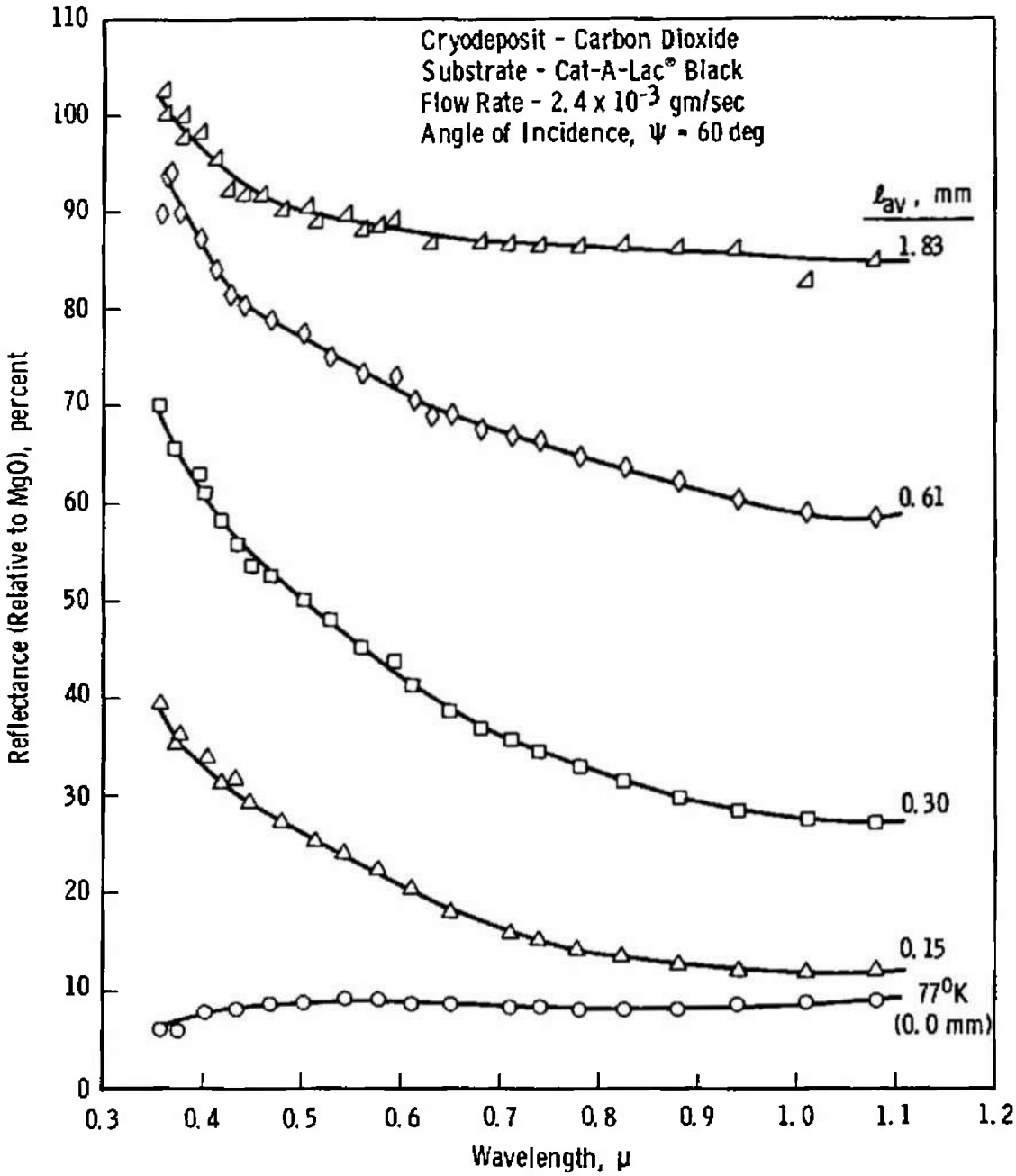

Fig. 16 Reflectance of Carbon Dioxide Cryodeposits on Cat-a-lac Black, ψ = 60 deg

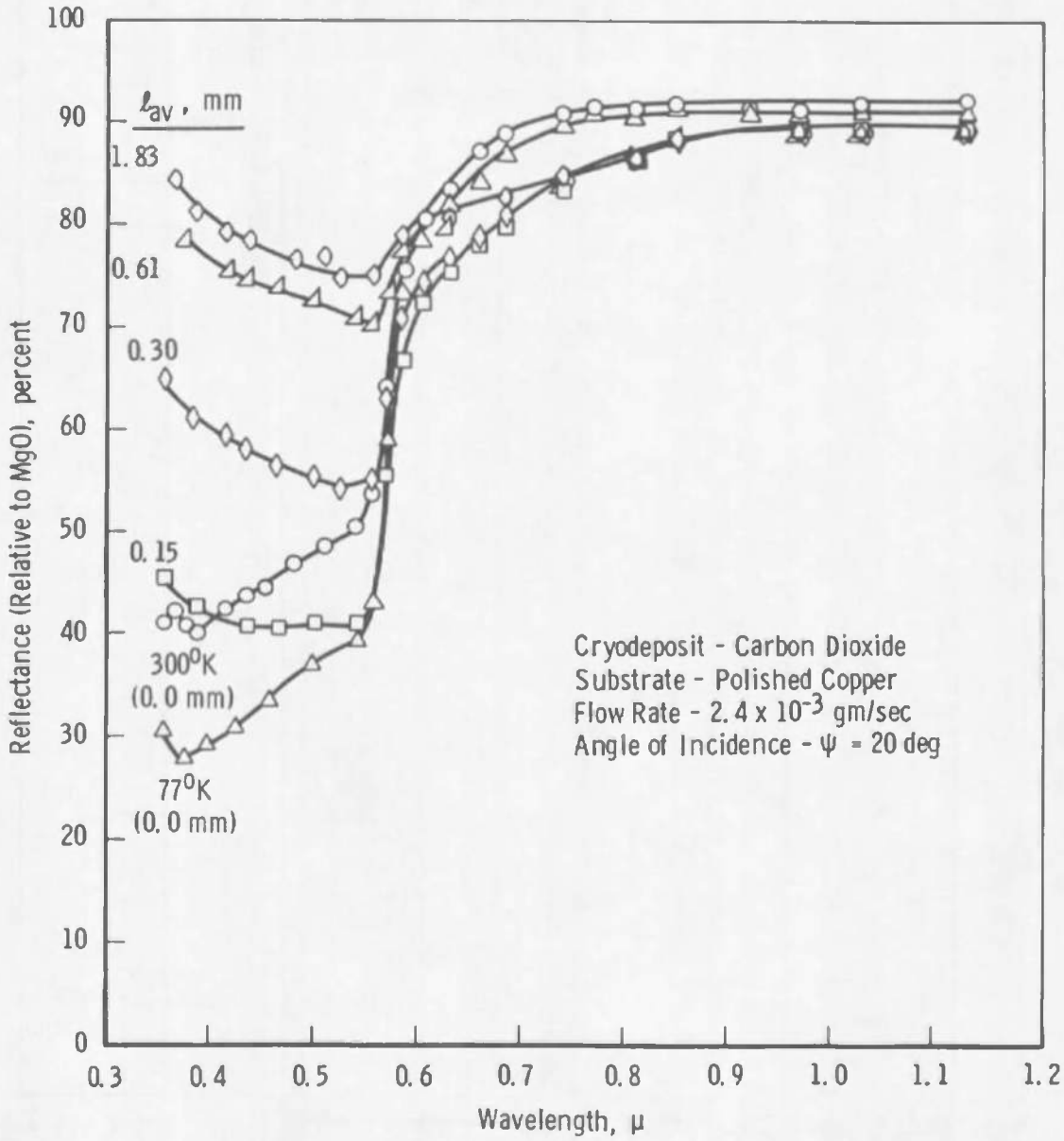

Fig. 17 Reflectance of Carbon Dioxide Cryodeposits on a Copper Substrate, ψ = 20 deg

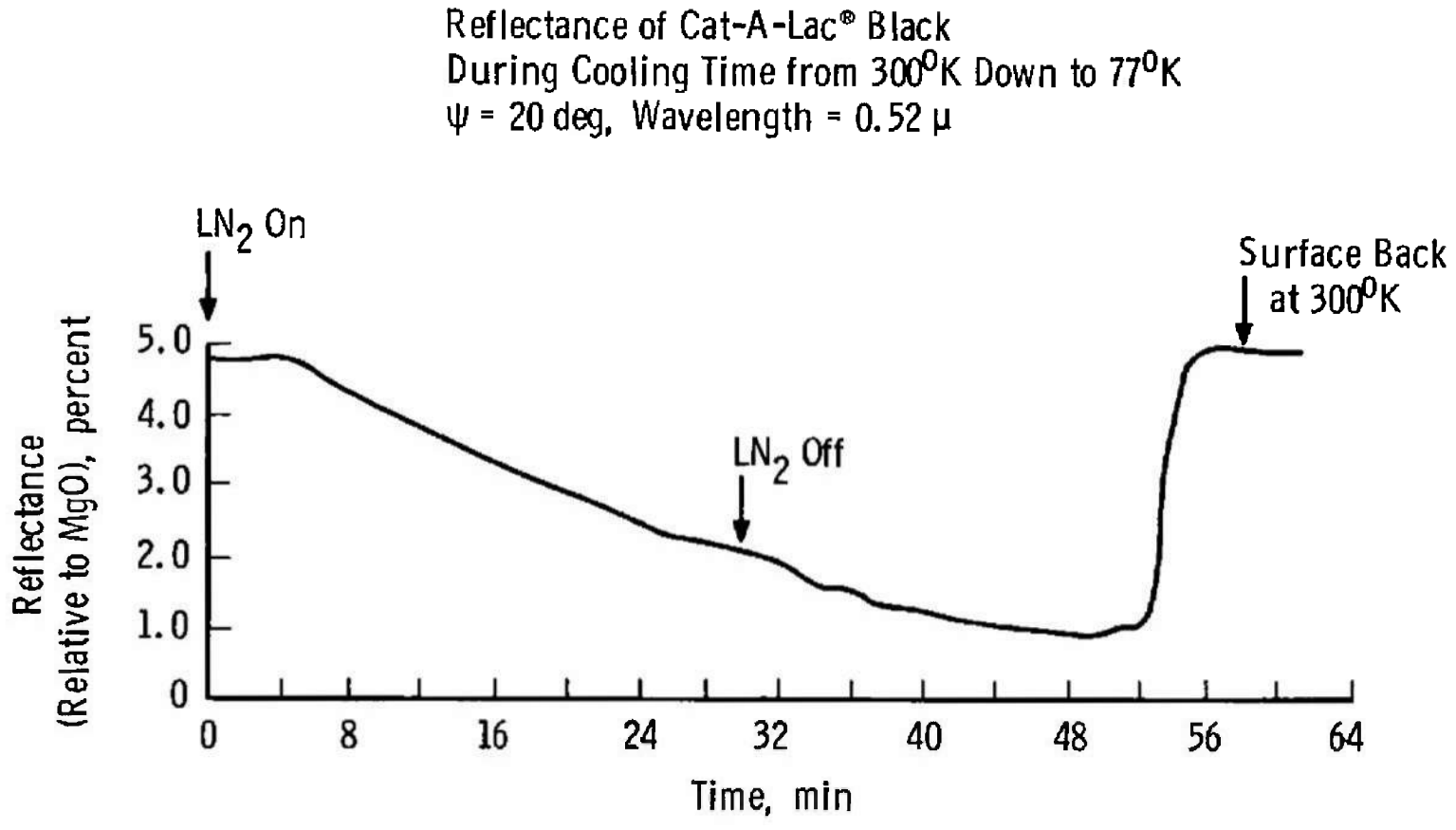

Fig. 18 Reduction in Reflectance of Cat-a-lac Black during Cooldown of Test Surface

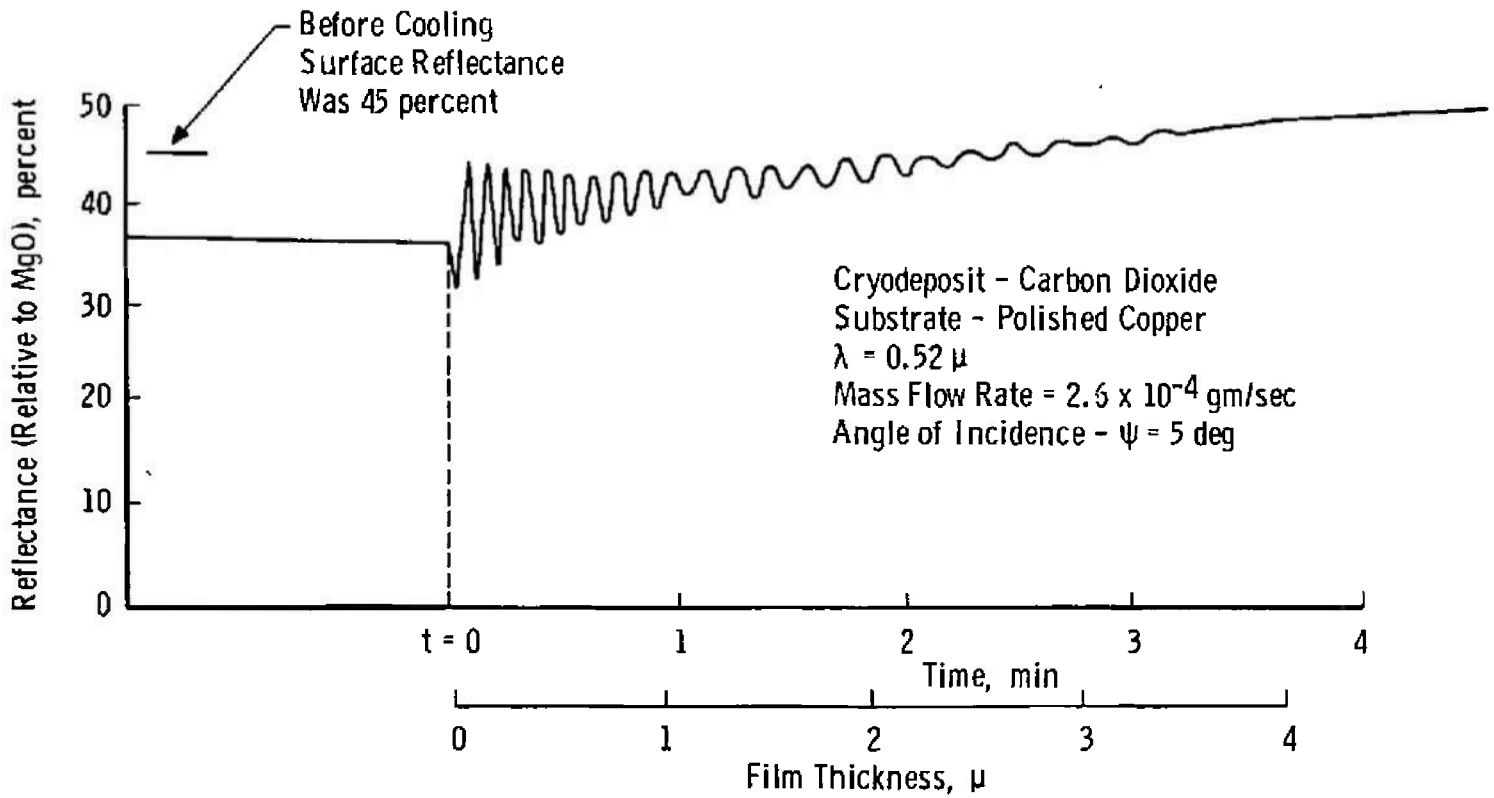

Fig. 19 Reflectance Patterns for a Thin Film of CO_2 Cryodeposit

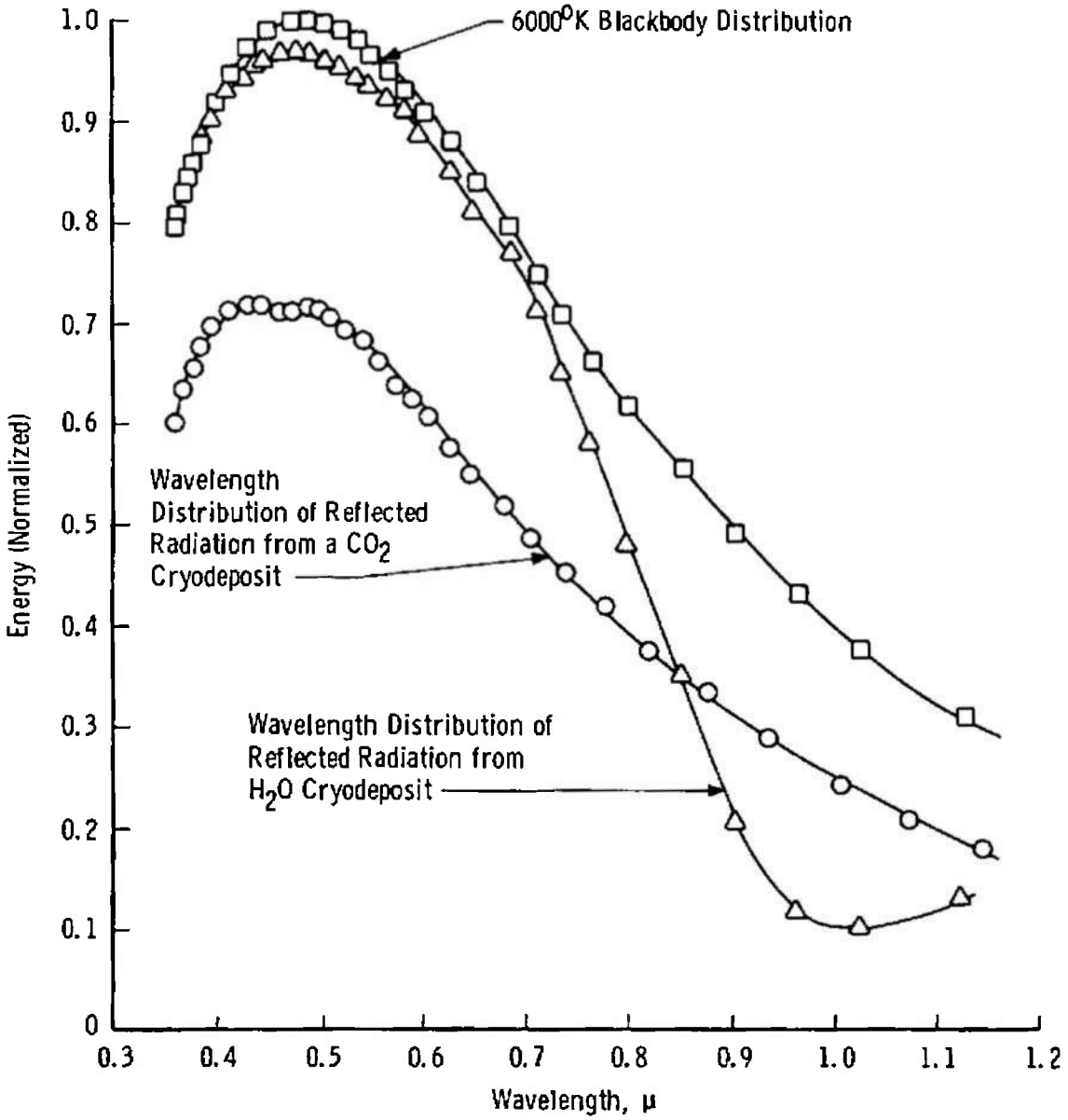

Fig. 20 Spectral Distribution of Reflected Energy from H_2O and CO_2 Cryodeposits 1.83 mm Thick Assuming a 6000°K Blackbody Source (ψ = 0 deg)

APPENDIX II
METHODS OF CALCULATION

The monochromatic radiant energy flux emitted by a blackbody at temperature T is given by Planck's spectral emittance equation (Ref. 12)

$$E(\lambda,T) = \frac{2\pi hc^2 \lambda^{-5}}{\exp\left(\frac{hc}{k\lambda T}\right)-1} \tag{II-1}$$

where c is the velocity of light, h is Planck's constant, and k is the Boltzmann constant. In this relation the constants $2\pi hc^2$ and hc/k are respectively referred to as C_1 and C_2, and their respective numerical values are 3.7413×10^{-12} w-cm^2 and 14,388 μ-°K. To obtain the radiant energy flux emitted by a blackbody within a particular wavelength interval, it is necessary to integrate the Planck equation in the following manner:

$$J(\lambda_1, \lambda_2, T) = \int_{\lambda_1}^{\lambda_2} \frac{C_1 \lambda^{-5} d\lambda}{\exp\left(\frac{C_2}{\lambda T}\right)-1} \tag{II-2}$$

The fraction of the total radiant energy flux which is contributed by the wavelength interval from λ_1 to λ_2, $f(\lambda_{12})$, can be found from the relation

$$f(\lambda_{12}) = \frac{\int_{\lambda_1}^{\lambda_2} \frac{C_1 \lambda^{-5} d\lambda}{\exp(C_2/\lambda T)-1}}{\int_0^{\infty} \frac{C_1 \lambda^{-5} d\lambda}{\exp(C_2/\lambda T)-1}} \tag{II-3}$$

In evaluating $f(\lambda_{12})$, the integrals are more conveniently handled if the change of variable

$$x = \frac{C_2}{\lambda T} \tag{II-4}$$

is introduced. Equation (II-3) can then be written as

$$f(x_i) = \frac{\int_0^{x_i} \frac{x^3 dx}{e^x - 1}}{\int_0^{\infty} \frac{x^3 dx}{e^x - 1}} \tag{II-5}$$

where $f(x_i)$ now represents that fraction of the total radiant energy flux which lies between x = 0 and x_i. These values of x correspond to a wavelength interval from $\lambda = \infty$ to λ_i. For further convenience the function $F(x_i)$ is defined such that

$$F(x_i) = 1 - f(x_i) \tag{II-6}$$

Then $F(x_i)$ obviously represents that fraction of the total radiant energy flux which lies between wavelength 0 and λ_i. Using this function, the fraction of the total radiant energy flux which lies between λ_1 and λ_2 can now be expressed as

$$f(\lambda_{12}) = F(x_2) - F(x_1) \tag{II-7}$$

In Ref. 11 the function $F(x_i)$ is computed for values of x between 0.7 and 36 in small intervals of x. It is also shown that a curve fit can be obtained for the function $F(x_i)$. This curve fit is expressed as

$$F(x) = e^{-x}(a x^3 + bx^2 + cx + d) \tag{II-8}$$

where the constants have the values

$$a = 0.15773679$$

$$b = 0.41286694$$

$$c = 1.0823067$$

$$d = 0.97180652$$

In the computer program the radiant energy flux within very small intervals was calculated using Eq. (II-8). For each λ and $\lambda + \Delta\lambda$, a corresponding x and $x + \Delta x$ can be found from Eq. (II-4). The fraction of the total energy within the wavelength interval $\Delta\lambda$ can then be found from $F(x + \Delta x) - F(x)$.

For example, consider the radiation energy flux in the wavelength interval from 0.36 to 1.15 μ. Assuming a 6000°K blackbody source and using Eq. (II-4), $x = 6.6983$ for $\lambda = 0.36\ \mu$ and $x = 2.0852$ for $\lambda = 1.15\ \mu$. Substituting these x values into Eq. (II-8) yields $F(2.0852) = 0.802$ and $F(6.6983) = 0.091$. These results indicate that 9.1 percent of the total energy from a 6000°K blackbody is of wavelengths less than 0.36 μ and 80.2 percent of this energy is of wavelengths less than 1.15 μ. Therefore, from Eq. (II-7), approximately 71 percent of this energy is within the wavelength range from 0.36 to 1.15 μ.

UNCLASSIFIED

Security Classification

DOCUMENT CONTROL DATA - R & D

(Security classification of title, body of abstract and indexing annotation must be entered when the overall report is classified)

1. ORIGINATING ACTIVITY (Corporate author)	2a. REPORT SECURITY CLASSIFICATION
Arnold Engineering Development Center ARO, Inc., Operating Contractor Arnold Air Force Station, Tennessee	UNCLASSIFIED
	2b. GROUP N/A

3 REPORT TITLE

THE SPECTRAL REFLECTANCE OF WATER AND CARBON DIOXIDE CRYODEPOSITS FROM 0.36 TO 1.15 MICRONS

4 DESCRIPTIVE NOTES (Type of report and inclusive dates)

Final Report. 1 May 1965 to 1 May 1967

5 AUTHOR(S) (First name, middle initial, last name)

B. E. Wood, A. M. Smith, and B. A. McCullough, ARO, Inc.

6 REPORT DATE	7a. TOTAL NO. OF PAGES	7b. NO. OF REFS
August 1967	45	12

8a. CONTRACT OR GRANT NO	9a. ORIGINATOR'S REPORT NUMBER(S)
AF 40(600)-1200 b. PROJECT NO. 8951 c. Program Element 6144501F d. Task 895104	AEDC-TR-67-131 9b. OTHER REPORT NO(S) (Any other numbers that may be assigned this report) N/A

10. DISTRIBUTION STATEMENT This document has been approved for public release and sale; its distribution is unlimited.

11 SUPPLEMENTARY NOTES	12. SPONSORING MILITARY ACTIVITY
Available in DDC.	Arnold Engineering Development Center (AETS), Air Force Systems Command, Arnold Air Force Station, Tennessee

13 ABSTRACT

The spectral reflectances of water and carbon dioxide cryodeposits were measured in a vacuum integrating sphere as a function of angle of incidence, substrate material, and cryodeposit thickness. Both Cat-a-lac® black paint and a polished copper surface were used as substrates. Measurements were made for wavelengths between 0.36 and 1.15 μ. Cryodeposit thicknesses ranging from 0 to 2.5 mm were investigated. For large cryodeposit thickness, the reflectance was, in general, increased considerably, especially for a Cat-a-lac black substrate. For thin cryodeposit thicknesses of less than 10 μ, interference patterns were observed. A computer program was written to calculate the energy reflected from cryodeposits for 6000°K blackbody irradiation. The reflectance data obtained in the present experiments may be useful for application to thermal models of planetary surfaces such as those of Mars and Venus.

This document has been approved for public release and sale; its distribution is unlimited.

DD FORM 1 NOV 65 1473

UNCLASSIFIED

Security Classification

UNCLASSIFIED

Security Classification

14. KEY WORDS	LINK A		LINK B		LINK C	
	ROLE	WT	ROLE	WT	ROLE	WT
1 spectral reflectance						
2 water cryodeposits						
3 carbon dioxide cryodeposits						
~~vacuum integrating spheres~~ 15-2						
4 substrates						
~~wavelength measurements~~						
5 Cryodeposits						

UNCLASSIFIED

Security Classification